



12-2003

Mechanical Properties and Corrosion Resistance of NI-SIC NANO Composite Coatings on 2024-T3 Aluminum

Amit Jain
Western Michigan University

Follow this and additional works at: https://scholarworks.wmich.edu/masters_theses



Part of the Engineering Science and Materials Commons

Recommended Citation

Jain, Amit, "Mechanical Properties and Corrosion Resistance of NI-SIC NANO Composite Coatings on 2024-T3 Aluminum" (2003). *Masters Theses*. 4762.

https://scholarworks.wmich.edu/masters_theses/4762

This Masters Thesis-Open Access is brought to you for free and open access by the Graduate College at ScholarWorks at WMU. It has been accepted for inclusion in Masters Theses by an authorized administrator of ScholarWorks at WMU. For more information, please contact wmu-scholarworks@wmich.edu.



MECHANICAL PROPERTIES AND CORROSION RESISTANCE OF NI-SIC
NANO COMPOSITE COATINGS ON 2024-T3 ALUMINUM

by

Amit Jain

A Thesis
Submitted to the
Faculty of The Graduate College
in partial fulfillment of the
requirements for the
Degree of Master of Science
Department of Materials Science and Engineering

Western Michigan University
Kalamazoo, Michigan
December 2003

Copyright by
Amit Jain
2003

ACKNOWLEDGMENTS

I would like to avail this opportunity to express my deep sense of respect and sincere admiration to my honorable thesis guide, Dr. Pnina Ari-gur for her tremendous efforts to guide me throughout this thesis. Her supervision, consistent guidance, co-operation proved to be the main drive behind completion of this thesis.

I would also like to thank my committee members Dr. Valery Bliznyuk, and Dr. Sam Ramrattan who took time out of their busy schedule and boosted my morale. I also thank Mr. Hussam Al-Khasawneh, Mr. John Cernius and Mr. Siddhartha Vemuganti for their timely assistance and consistent support without which this project would have been a lot for me. I take this opportunity to thank Mr. Seyed Mirmiran, Daimler Chrysler, Mr. Wei Ren, Oakland University, Dr. Daniel Khujawski, Mr. Stoyan Stoychov and Mr. Siddhartha Vemuganti for extending their helping hand and the facilities for our experiments, and I really appreciate their goodwill and camaraderie

This acknowledgement would be incomplete without thanking God, my parents, my roommates, and my loved ones for their continued confidence and unconditional love for me.

Thank you all.

Amit Jain

MECHANICAL PROPERTIES AND CORROSION RESISTANCE OF NI-SiC NANO-COMPOSITE COATINGS ON 2024-T3 ALUMINUM

Amit Jain, M.S.

Western Michigan University, 2003

Coatings of nickel with and without silicon carbide nano-particles were carried out on 2024-T3 aluminum alloy by the electrochemical process. The size of the silicon carbide particles was less than 50nm. Nickel coatings were done using a nickel sulfamate bath maintained at a constant temperature of $50^{\circ} \pm 5^{\circ}$ C. Tensile specimens were prepared and studied to determine the Young's modulus of bare aluminum, with nickel coatings and with composite nickel and silicon carbide coatings. Wear samples of 1 inch² (6.45cm²) were prepared and studied for wear resistance. The residual stress measurements were done by the hole drilling method and were compared with bending due to tension. Potentiodynamic corrosion tests were carried out to study the corrosion rates of bare aluminum and that of 50 microns and 208 microns nickel only samples. The thickness of the coatings was determined using scanning electron microscope. The stiffness of the samples increased with the increasing silicon carbide content to 21 g/L. the corrosion resistance and the wear resistance increased with nickel coating. Tensile residual stresses were found in the coating.

TABLE OF CONTENTS

ACKNOWLEDGMENTS	ii
LIST OF TABLES	vi
LIST OF FIGURES.....	vii
CHAPTER	
I. INTRODUCTION.....	1
1.1. The need for coatings	1
1.2. Nanocomposite.....	4
1.3. Electroplating	5
1.3.1. Basic process.....	5
1.3.1.1. Hydrogen evolution and cathode efficiency	6
1.3.1.2. Anode efficiency.....	6
1.3.1.3. Nickel ion and pH changes.....	7
1.3.1.4. Amount of nickel deposited.....	7
1.4. Nickel	8
1.4.1. Nickel anode materials.....	9
1.5. Residual stress.....	10
1.5.1. Methods of residual stress determination	11
1.5.2. Hole drilling method.....	11
1.6. Corrosion studies.....	12
1.6.1. Polarization studies.....	14
1.7. Tensile tests	14

Table of Contents—continued

1.8. Wear tests	16
1.8.1. pin-on-disk method	16
II.EXPERIMENTAL PART	19
2.1. Nickel electroplating	19
2.2. Pre-coating.....	20
2.3. Final coating	24
2.4. Experimental setup	31
2.5. Equipment	31
2.6. Chemicals	38
2.7. Residual stress hole drilling	44
2.7.1. Procedure	44
2.7.2. Installation of the strain gage	45
2.7.3. Specifications	46
2.8. Evaluation of stress in metallic films deposited by electrolysis using the bending method	53
2.9. Corrosion (potentiodynamic) setup	54
2.9.1. Run parameters	55
2.9.2. Sample parameters	56
2.10. Tensile tests	57
2.11. Wear tests	57
2.12. Sample and the coating parameters	59
2.12.1. Tensile samples.....	59
2.12.2. Rectangular samples	59

Table of Contents—continued

III.EXPERIMENTAL RESULTS	60
3.1. Dimensions of tensile specimens	60
3.2. Residual stress results.....	61
3.2.1. Hole drilling.....	61
3.2.2. Bending due to tension.....	64
3.3. Corrosion tests (potentiodynamic)	64
3.4. Tensile tests.....	68
3.5. Wear test results	70
IV.DISCUSSION.....	78
V. CONCLUSION.....	81
VI. REFERENCES	82
APPENDICES	
A. Suppliers	86
B. Tensile test plots	88
C. Minitab plots for tensile tests.....	92
BIBLIOGRAPHY	97

LIST OF TABLES

1. Properties of aluminum alloy 2024.....	2
2. Basic information about nickel	8
3. High throwing power nickel electroplating and its applications.....	42
4. Specifications of the CEA-XX-062-UL-120 strain gage rosette	46
5. Dimensions of the tensile specimens	60
6. Measured strains and relieved strains	61
7. Calculated values of coefficients	62
8. Measured residual stresses and their orientation.....	63
9. Corrosion rate values for the samples	68
10. Combined table for Young's modulus.....	69
11. Nickel – 7g/L SiC coated sample.....	70
12. Nickel only sample.....	73
13. Nano silicon carbide specifications.....	77

LIST OF FIGURES

1. Stress-strain diagram	15
2. Coated sample in the pin-on-disc setup	17
3. Pin-on-disc setup.....	17
4. Pre-coating sequence for aluminum alloys	21
5. Electrochemical cell.....	25
6. Effect of cathode shape on current distribution	27
7. Hot plate.....	31
8. Heating element	31
9. Coating bath	33
10. Heating element and heating controller for the coating bath	34
11. Power source	35
12. Nickel anode	36
13. Anode bag	36
14. Cathode holder	37
15. Air flow meter and controller.....	38
16. Bubblator.....	38
17. Precoating assembly	39
18. CEA-XX-062UL-120 special rosette strain gage.....	45
19. Degreaser	47
20. Adhesive kit and preserve coat	49
21. Gage assembly	50

List of Figures—continued

22. Hole drilling setup I	50
23. Gage assembly in the setup	51
24. Hole drilling setup II	51
25. Switch balance units	51
26. Drilled hole	52
27. Coated sample showing the bending.....	53
28. Potentiodynamic setup	54
29. The 5-neck cell.....	54
30. Potentiodynamic output	56
31. Tensile test setup.....	57
32. Aluminum in 0.6M NaCl	65
33. Nickel 50 microns in 0.6M NaCl.....	66
34. Nickel 208 microns in 0.6M NaCl.....	67
35. Young's modulus comparison for the samples	69
36. Friction force vs. sliding speed plot for Ni-7g/L SiC sample	72
37. Wear track image for Ni-7g/L SiC sample	72
38. Friction force vs. sliding speed plot for Ni only sample.....	75
39. Wear track image for Ni only sample	76
40. Comparison of friction force vs. sliding speed for Ni SiC & Ni only sample	76
41. SEM micrograph 208 microns nickel coating.....	77

CHAPTER I

INTRODUCTION

1.1. The need for coatings

There are various reasons to use different alloys in the industry today. Some of the reasons for the use of aluminum alloys, viz. Al 2024-T3, include appreciable reduction in weight without compromising strength, and also requirement for minimum maintenance. These advantages are coupled with their ease of fabrication to get them into desired shape.¹

In the aerospace industry, thin sheets of Al 2024-T3 of 0.063" (0.16 cm) have been used extensively in the later half of the 20th century. This might be attributed to their availability, chemical stability, low density and high specific elastic modulus. Aluminum has a density of 2.77 gm/cm³ and an elastic modulus of 70 GPa as compared to steel which has a density of 7.86 gm/cm³ and elastic modulus of 210 GPa. The basic composition of Al 2024 alloy includes 4.5% Copper, around 0.6% Manganese, and around 1.5% Magnesium.²

Though this alloy has excellent physical and mechanical properties, the corrosion resistance takes a back seat due to the presence of copper. The corrosion gets accelerated due to the presence of galvanic pair of aluminum and copper. In any galvanic pair, the metal near

the top of the galvanic series will be the anode and will ionize and go into the solution or corrode, while the one closer to the bottom of the series will be the cathode and receive galvanic protection. The speed at which galvanic corrosion takes place depends entirely on the difference in the electrical potential between the two metals. Aluminum (-0.76v) coupled with copper (-0.36v) will have a corrosion potential of over 400 milivolts. ⁴

The physical properties of the 2024 aluminum alloy are summarized in Table 1, as follows:

Table 1: Properties of aluminum alloy 2024³

Yield Strength (Typical for –T3)	290	MPa
Tensile Strength (Typical for –T3)	434	MPa
Young's Modulus	73	GPa
Shear Modulus	28	GPa
Poisson's Ratio	0.33	
Thermal Expansion Coefficient	22.7	E-6 1/C
Density	2768	kg/(m ³)
Thermal Conductivity	121	W/(m-C)
Specific Heat	0.963	kJ/(kg-C)
Melting Point	638	C

Since such corrosion coupled with high-cycle fatigue as in the case of an airplane can be detrimental, therefore it is imperative to protect the alloy by the means of noble coating.⁵

In recent years, a lot of importance and work have been put into developing metal-matrix composite coatings containing ceramic particles, as they have better corrosion resistance and better wear-resistance properties than the uncoated metal and a lot of metallic matrices have been co-deposited with a wide variety of hard or lubricating particles, like, carbides, oxides, PTFE, graphite etc.⁶

Nickel coating and nickel nano-composite coatings are being studied and applied commercially in a successful manner due to the low cost of the ceramic powder and high wear resistance.⁷

Aluminum-based metal matrix composites are widely researched nowadays because of their improved specific strength, excellent wear resistance, higher thermal conductivity than ceramics and lower coefficient of thermal expansion.⁸

Electro-deposition will result in nano-structured materials when the process parameters e.g. bath composition, pH, temperature, over potential, are chosen such that electro-crystallization results in massive nucleation and reduced grain growth.⁹

This process is relatively inexpensive, is easy to apply at relatively low temperatures and also on a variety of complicated geometries.

Due to the existence of non-metallic inclusions in the metallic matrix, there are changes in the mechanical and physical properties of the material. Therefore, it becomes necessary to study the changes in the wear resistance, residual stresses, along with the stiffness of the electroplated material and the corrosion resistance of the material.

1.2 Nanocomposite¹⁰

The conventional definition of nanomaterials is “a material having a characteristic length scale of less than about a hundred nanometers. This length scale could be particle diameter, grain size, layer thickness, or width of a conducting line on an electronic chip.”

Technologically useful properties of nanomaterials are not limited to their structural, chemical or mechanical behavior. New processes to produce large quantities of nanomaterials and to better characterize these materials have been established. Each fabrication technique has its own set of advantages and disadvantages. Generally it is best to produce nanomaterials with a narrow particle size distribution.

Free jet expansion techniques permit the study of very small clusters. Its only disadvantage is producing a small quantity of material. Mechanical attrition, which can also produce a large amount of material, often makes less pure material.

The different methods used for the formation of larger nano-particles are sputtering, thermal evaporation and laser method.

There are two major differences between the nano-particles and the clusters. First, nano- particles produced directly from a supersaturated vapor are usually larger than the clusters. They range in size from 1 to 100 nm. Secondly, the nano-particles are usually produced in much larger quantities than the clusters produced in a free jet expansion.

1.3 Electroplating¹¹

Nickel plating is a widely used industrial process for aesthetics and engineering purposes. The main reason is that the processes can be fine-tuned considerably with slight modifications in composition and the operating parameters of the electroplating solution. Nickel plating deposits or coatings may also be incorporated to modify and or to improve the mechanical and physical properties of the base metal, such as corrosion and wear resistance and possibly as a barrier in electrical and electronic applications for other industrial purposes. The industrial nickel plating deposits are generally not bright and shiny, but rather matte finish in appearance, whereas, the decorative nickel deposits acquire their bright finish directly from the nickel plating solution. Nickel plating is metallurgically bonded to the base metal substrate, nickel shares electron with aluminum in our case, and is an integral part of the assembly surface after the process completion.

1.3.1 Basic process¹¹

Nickel plating, as other prominent electroplating processes, makes use of soluble metallic anodes based on the universal reduction and oxidation (redox) reaction. As an important step in an electrochemical process, a direct current (DC) is passed between the

anode and the cathode through a conductive aqueous nickel salt solution. Due to the redox reaction, anode dissolves and the cathode is plated with the anode ions.

“The nickel in the solution is made of divalent positively charged ions (Ni^{+2}). During the current flow, the positive ions react with two electrons and are converted to metallic nickel (Ni^0) at the cathode surface”.

1.3.1.1. Hydrogen evolution and cathode efficiency ¹¹

Cathode efficiency during the electro-deposition process is reduced by approximately 3-8% and is dependent on the electrolyte nature. Cathode efficiency is reduced due to the consumption of direct current, during the hydrogen ion discharged from water in the process.

1.3.1.2. Anode efficiency ¹¹

Similar to the cathode efficiency, anode efficiency is an important process variable in the electroplating process. pH of the electrolytic solution plays an important role in the determination of anode efficiency and has to be maintained throughout the process in order to achieve maximum anode efficiency. In the case of a nickel anode, the discharge of oxygen may contribute to the passivity of nickel anode which may impede any further oxidation reaction, thus ceasing the anode to dissolve any further.

Commercially available “activated” nickel anodes resist this passivity onset and hence provide for a smoother operation, by maintaining the anode efficiency as close to maximum as possible.

1.3.1.3. Nickel ion and pH changes ¹¹

As the electroplating process continues, the pH of the conductive aqueous solution tends to increase slowly with a similar increase in the concentration of nickel ions, depending on the inherent anode and cathode efficiencies. Per earlier discussions, as these efficiencies may vary and may not be at 100% at all the times, the nickel ion concentrations and the pH change rates don't depend upon the anode material in use but rather on the nature and characteristics of the plating solution

1.3.1.4. Amount of nickel deposited ¹¹

The Faraday's law, for calculating the amount of nickel deposited on cathode, can be expressed as;

$$m = 1.095 (a) (I) (t) \text{ }^{11}$$

Where:

m = amount of nickel deposited at the cathode (grams)

a = current efficiency ratio

I = current that flows through the plating tank (amperes)

t = time that the current flows (hours)

In most cases, the current efficiency is 100% ($a=1$). The cathode efficiency may vary from 92-97% and accordingly, a will vary from 0.92 to 0.97. As is evident from the Faraday's law the amount of nickel deposited on the cathode is in direct proportion to the product of current and time.

1.4. Nickel ¹¹

Table 2: Basic information about nickel ¹¹

Symbol	Ni
Atomic weight	58.69
Valency	2
Specific gravity	8.90
Plating rate, at 100%	1.095 g/Ampere-hour
Cathode efficiency	0.039 oz. /Ampere-hour

At the conditions of cathode efficiency of 95.5%, at $5\text{A}/\text{dm}^2$, it should take about 20 minutes to deposit a nickel coating with an average thickness of 20 micrometers.

Nickel sulfamate solutions are widely used for electro-forming, the production of components by electro-deposition on a mold which is finally separated from the coating, because of the low internal stress of the deposits, high rates of deposition, and superior throwing power. Throwing power is the relationship between the current distribution and uniformity of coating thickness. Because of the high solubility of nickel sulfamate, a higher nickel metal concentration is possible than in other nickel electrolytes, permitting lower operating temperatures and higher plating rates.

Nickel sulfamate is highly soluble so that it cannot be readily crystallized from solution. It is commercially available as a concentrated solution usually prepared by reacting high purity nickel powder with sulfamic acid under controlled conditions. This solution is more expensive than other solution available but extra cost of using the solutions that are as pure as possible is more than offset by savings in the preliminary purification procedures necessary otherwise.

1.4.1. Nickel anode materials¹¹

Most nickel plating processes are operated with soluble nickel anode materials. Nickel from the anode is converted into ions that enter the plating solution and

replace those discharged at the cathode. The anode distributes current to the parts being plated and influences metal distribution. The simplest way to satisfy anode requirements is to suspend nickel bars from hooks placed on an anode bar, so that nickel, and not the hook, is immersed in the plating bath.

1.5. Residual stress ¹²

It is well established that virtually no material, no component and no structure of technical importance exists free of residual stresses. Residual stresses are produced if regions of a material are inhomogeneously elastically or plastically deformed in such a permanent manner that incapability of the state of deformation occurs. Especially in structural parts, a great variety of the residual stress states can exist as consequences of various technological treatments and manufacturing processes. All stress states within a material which are independent of the outside forces are called residual stresses. Residual stresses can occur due to various reasons as material processing.

Progress in the material science and technology has lead to new challenges for residual stress analysis. Studying of residual stresses especially after various mechanical surface treatments has really become of prime importance.

In the electroplating process though there is no applied mechanical load, these stresses are a result of the coating nature and the chemical media used for the coating. This is because this medium will affect the way the grains are stacked on the surface of the sample substrate.

Residual stresses measurement is an indirect method. They are calculated by measuring strain from which the stress is calculated using the elastic constants of the material, or by a calibration procedure – involving measurement of strain produced by known stress.

1.5.1. Methods of residual stress determination

Several methods are used for the determination of residual stresses. They can be categorized into two main subdivisions as destructive techniques and non destructive techniques. The main difference between these two is, that in destructive techniques the sample has to be mechanically destroyed, and is not fit for mechanical use after the test. Non destructive tests are often done on-site and they have no effect on the mechanical operations of the component tested.

1.5.2. Hole drilling method ²⁴

The bonded electrical resistance strain gage is widely recognized as the most practical technology for testing of load-bearing parts, members, and structures because both

excellent accuracy and repeatability can be achieved. In order to measure the residual stresses with the standard sensors, the locked-in stress must be relieved in some fashion (with the sensor present) so that the sensor can register the change in the strain caused by removal of the stress. With strain sensors judiciously placed before dissecting the part, the sensors respond to the deformation produced by the relaxation of the stress with material removal. The initial residual stress can then be inferred from the measured strains by elasticity considerations.

1.6. Corrosion studies¹³

Corrosion is a deterioration and/or destruction of the metal because of the reaction with the environment. It can also be explained as the loss of useful properties of the material as a result of the chemical or electrochemical reaction with the environment.

It is important to study corrosion due to several reasons. Some of them include the increasing use of the metals and alloys in all the fields of technology, use of rare and expensive materials whose protection require special attention, use of new high strength alloys whose susceptibility to certain types of corrosion attack is more, increasing pollution of the air and water, strict safety standards of the operating equipment, and not the least due to the increasing awareness of the need to conserve world's metal resources.

From an engineering point of view, the major interest is in the kinetics or the rate of corrosion. Corroding systems are not at equilibrium, and therefore thermodynamics calculations are not valid here.

Definitions:

Anode: Electrode at which net oxidation occurs

Cathode: Electrode at which net reduction occurs

Polarization: Displacement of the electrode potential resulting from a net current. Polarization can be divided into activation, concentration and resistance polarization. The magnitude of the polarization is often measured in terms of overvoltage. Overvoltage is a measure of the polarization with respect to the equilibrium potential of an electrode.

Corrosion rate is usually expressed as mils penetration per year (mpy) or millimeters per year (mmpy).

$$1 \text{ mpy} = 0.805 \text{ pm/sec}$$

Where; 1 picometer = 10^{-12} meters.

$$\text{Corrosion rate (mpy)} = (1.24 \times 10^7 \text{ We/icorr})/\text{density}$$

Where we = electrochemical equivalent (mg/coulomb)

Two main techniques used for the corrosion rate determinations on the laboratory scale are; Weight loss method and Polarization method.

1.6.1. Polarization studies

In the potentiostatic method, the electrode potential of the material is changed either manually, or automatically using an electronically-controlled instrument known as potentiostat and the current flowing in the external circuit is recorded with respect to time.

1.7. Tensile tests ¹⁴

Strength of a material depends on its ability to sustain load without permanent deformation or fracture. This property is inherent in the material itself and must be determined by experiments. One of the most important tests to perform in this regard is the tension or compression test. Although many important mechanical properties of a material can be determined from this test, it is used primarily to determine the relationship between the average normal stress and average normal strain in many engineering materials such as metals, ceramics, polymers, and composites. To perform the tension test, a specimen of the material is made into a standard shape and size. Before testing, two small punch marks are identified along the specimen's length. These marks are located away from both ends of the specimen because the stress distribution is somewhat complex due to the gripping of the connections where the load is applied.

A compression/tension testing machine is usually used for carrying out the experiment. The specimen is stretched at a very small constant rate until it reaches the breaking point. The machine is designed to read the load required to maintain this uniform stretching. At frequent intervals during the test, data are recorded of the applied load P , as read on the dial of the machine or taken from a digital readout. Also the elongation $\Delta L = L - L_0$ between the punch marks on the specimen may be measured using a caliper or an optical device called an extensometer. The strain sensors are attached to the specimen gage length to get the values of the strain in the elastic range, which otherwise might be lost in the process.

Stress; $\sigma = P/A_0$; P is applied load, and A_0 is the original cross sectional area.

Strain; $\epsilon = \Delta L/L_0$; ΔL is change in specimen's gage length, and L_0 is the original gage length.

Shown below is an example of stress-strain diagram ¹⁵

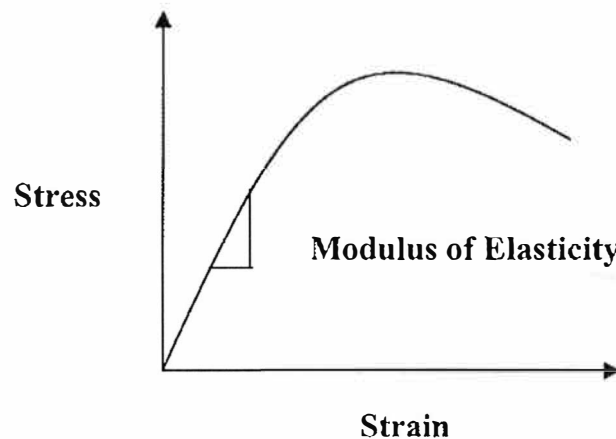


Figure1: Stress-strain diagram

If the corresponding values of σ and ϵ are plotted as a graph, for which the ordinate is the stress and the abscissa is the strain, the resulting curve is called as conventional stress-strain diagram. This curve is shown above in Figure 1. This diagram is very important in engineering since it provides the means for obtaining data about a material's tensile strength without regard for the material's physical size or shape.

The ratio of stress and strain is taken in the elastic zone, or in other words, the slope of the linear line of the elastic zone is taken to calculate the Young's modulus or the stiffness of the material.

1.8. Wear tests¹⁶

In general, there are four different types of wear in the machinery: adhesive, abrasive, erosive and fretting. Adhesive wear results from the adhesion between two sliding surfaces. These two surfaces start to wear and particles are released from the two surfaces as wear debris. Abrasive wear occurs, when a sharp object is pressed onto another surface.

1.8.1. Pin-on-disc method

The pin-on-the disk method is done in accordance to the test method for wear testing with a pin-on-disk apparatus, ASTM designation on: G 99-95a, pp. 1-5, 2000.¹⁵

Shown in Figure 2 and Figure 3, is a typical setup for the pin-on-disc method. Figure 2, shows a sample in the assembly and Figure 3 shows the basic setup in terms of dead weight and data acquisition.

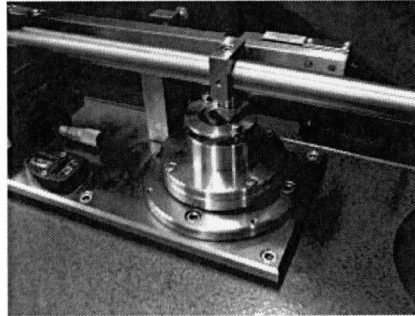


Figure 2: Coated sample in the pin-on-disc setup¹⁶

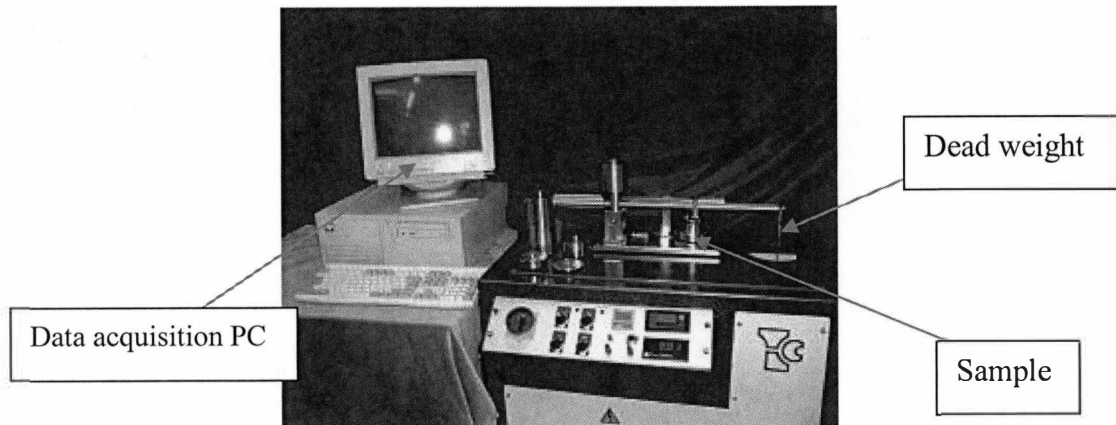


Figure 3: Pin-on-disc setup

The pin-on-disc method of wear test uses a high-torque drive motor to rotate a flat sample under a loaded wear pin. The wear pin is a 5 mm diameter ball made either from chromium steel or tungsten carbide-cobalt. The wear pin creates a circular track of the required diameter by offsetting the pin relative to the sample's centre of rotation. Due to the

sliding motion of the sample under the wear pin, frictional force which is property of the film is given, and this is proportional to the load applied. The examination of the resulting plot of friction versus time gives an indication of the friction characteristics and endurance of a particular coating. The test will automatically be stopped if the maximum friction force or maximum time is reached. The time at which coating failure occurs is usually indicated by a rise in the friction.¹⁷

CHAPTER II

EXPERIMENTAL PART

2.1. Nickel electroplating ¹⁷

The coating process of nickel on aluminum substrate is a two-step process. This is divided into two main divisions, Precoating and Final Coating. Aluminum has a basic tendency to form an oxide layer of alumina (Al_2O_3), immediately when exposed to the atmosphere. The Al_2O_3 film is good for the corrosion resistance of aluminum; however, it makes it impossible to coat aluminum with any other metal directly. In order to prepare aluminum for the nickel coating, it is necessary to get this film of Al_2O_3 destroyed or changed into some other chemical nature. This is one of the main reasons for the process of precoating.

Proper surface preparation prior to plating is critical to obtaining a quality plating deposit. A number of process cycles, cleaners, acids, and specialty formulations are available. The selection of the proper cleaning, pickling, and activation cycle as well as selection of specific materials and solution compositions is crucial and deserves careful consideration.

In the process of precoating, the aluminum substrate goes through a series of unit operations, which introduce it to various chemical treatments. The main objective of these unit cell operations is to clean and change the chemical nature of the aluminum substrate surface, which in turn will facilitate the coating of nickel on it. This is mainly done with Bondal process, without applying brass or copper plating. This treatment produces a film on aluminum alloys, which may be plated directly with nickel, copper, brass, silver, chromium, tin, zinc or cadmium.

Engineering nickel plate has a matte finish and is used to alter or enhance characteristics such as corrosion resistance, wear, hardness and magnetic properties of the substrate. Other applications include repair, rebuilding, and salvage of various machine parts, and heavy undercoating for hard chrome plating.

2.2. Pre-coating

As already discussed, precoating is a very important intermediate step in any metallic coating on aluminum sample. Obvious reasons include the alumina film that's formed on the surface of aluminum substrate, when it comes in contact with the atmosphere and reacts with the oxygen in the atmosphere.

Precoating sequence of 2024-T3 aluminum alloy is shown in Figure 4. ¹⁸

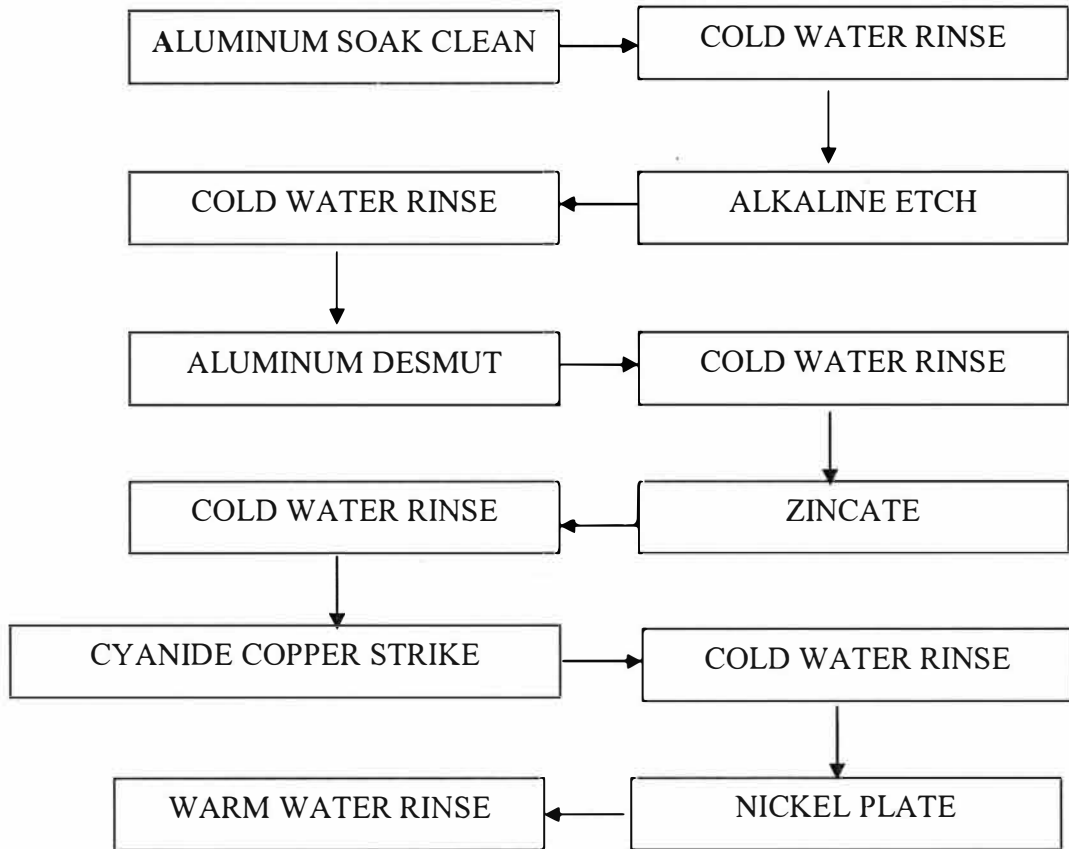


Figure 4: Pre-coating sequence for aluminum alloys

Cold water rinse was done using the De-ionized water

Precoating is composed of four separate operations, as follows;

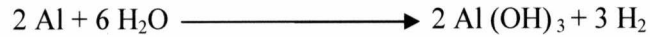
- Alkaline Degreaser

The aluminum substrate that has to be coated must have passed a series of manufacturing processes. These may include rolling, stamping, machining, grinding or finishing. Due to one of these or their combinations, the aluminum substrate would have some debris, or dust/dirt and also some polymers as well that might include grease, oil and paints. The surface of the substrate has to be perfectly clean in order to minimize the variables for a perfect coating. These impurities on the substrate may have a substantial effect on the coating of the nickel layer and also the adhesion of the same on the substrate. Therefore it is essential to get rid of this layer of impurity. Hence the use of an alkaline degreaser is made. In the case of our experiment we have used a solution of Disodium Trioxosilicate. This solution is corrosive in nature and it converts the grease and dirt from insoluble to soluble compounds due to saponification. Also the pH of the solution should be around 9-11.

- Alkaline Etching

As already discussed, the oxide layer of the aluminum has to be removed before depositing the nickel. The oxide layer that covers the substrate is destroyed

by alkaline etching and a smooth layer of aluminum hydroxide is formed due to the following chemical reactions taking place.



These reactions are exothermic. In addition hydrogen gas evolves from the reactions. Aluminum does not react with water directly, since the oxide layer that cover the aluminum is not permeable and then it protect the aluminum. The formation of this protective layer is prevented by the formation of $[\text{Al} (\text{OH})_4]^-$ which is an amphoteric compound, that is it has the capability of reacting in acidic and basic media. Aluminum hydroxide dissolve in the solution and aluminum oxide layer also demolished according to the following reaction:



- Acidic Etching

The main objective for this operation is to give a good finish to the surface of the aluminum substrate by removing any final oxide layer or dirt/grease from the surface of the sample before applying the coating. A solution of 25% HCl + 25% HNO₃ in 50% water is used for the purpose.

The reactions of HCl and HNO₃ with aluminum are as followed:



- Zincate

This is the most important step in pre-coating., because this prepares the surface of the aluminum substrate for the final nickel coating. Nickel will not deposit directly on oxide or metallic surface and hence this stage gains its importance. It is generally recommended to apply the zincate twice on the surface. The first layer being thick and porous, this will dissolve in acidic media. Second layer should be smooth, with less porosity.

2.3. Final coating

Once the 2024-T3 aluminum substrate is ready for the final coating of nickel, it is shifted to a nickel coating bath, which comprises of an electroplating cell as one shown below in Figure 5.

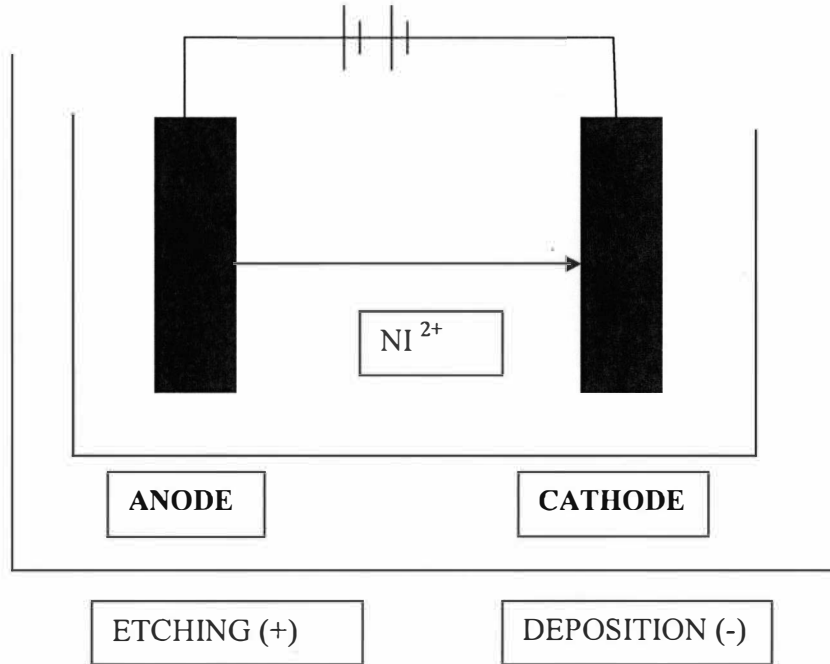


Figure 5: Electrochemical cell¹⁹

Electroplating is described as the electrolytic deposition of a metal from a solution onto the surface of a substrate immersed in that solution.

The *plating bath* is a solution of metallic ions or salts dissolved in an acid or alkaline base. The part to be plated is submerged in the bath and an electric current is applied. The part is usually situated in the center of the plating tank, and acts as the cathode. The anodes are positioned near the edges of the tank. A rectifier, or generator, is used to produce the electric current. The electrons travel in a path from the rectifier to the cathode, through the bath to the anode, and finally back to the rectifier. This movement causes the positively

charged metal ions in the bath to migrate toward extra electrons located at the cathode (the part to be plated). The electrons neutralize the positive charge of the metal ions, causing a film of the metal to adhere to the cathode. Thus a thin coating of the metal in the solution forms on the surface of the part.²⁰

Nickel plating is defined as electrolytic deposition of a layer of nickel on a substrate. This involves the dissolution of the anode (nickel) and deposition nickel on the surface of another metal through an aqueous solution of the metal salt, nickel sulfamate, which will act as a salt bridge and also provide the needed conductivity to transfer the ions from the anode to the cathode. Also a direct current is applied through the anode and cathode. Theoretically the coating process can go for ever without interruption even after the Ni anode is fully consumed.²⁰

The adhesion of the nickel layer and the thickness of that layer are important in the determination of the quality of the coated layer. The porosity and thickness distribution through the surface are also important. The factors that control the quality of the coating are current density, duration of coating, pH of the coating bath and mixing rate.²⁰

It is believed that the acidity of the bath affect the quality coating, since it was found by measurements that the pH of the solution changes as the coating proceeds. To eliminate the effect of pH change, it should be monitored and controlled. We used sodium hydroxide mixed with 10 ml of water to control the pH of the solution in our experiment. Anode and cathode placement in the solution is also important to control the thickness and uniformity of

the coated nickel, the best setting of cathode and anode found by trial and error of a specific setting. The geometrical shape of the anode and cathode also affects the coating thickness and distribution.²⁰

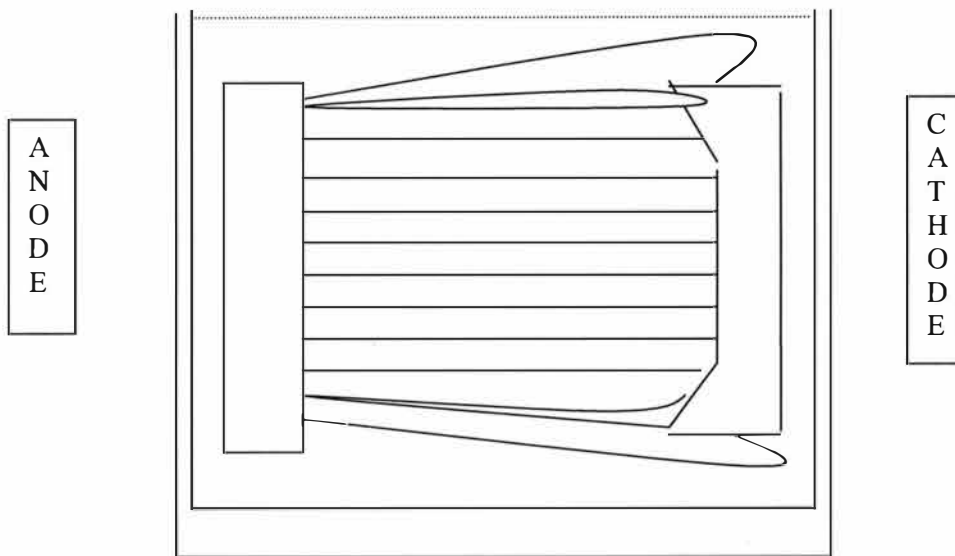


Figure 6: Effect of cathode shape on current distribution

The Figure number 6 above shows the effect of Cathode Shape on Current Distribution. Shows how the shape of the cathode can affect the distribution of current density and then the thickness of the coated layer.

The shape of the part can influence the thickness of the deposited metal. Shapes such as open containers when plated with certain solutions will tend to have thicker deposits on

the outside corners, and thin deposits on the inside corners. The difference in plating thickness can be as much as five times thicker on the outer edges. This occurs because the current flows more densely around the outer corners than on the inner corners.²⁰

Some plating solutions do not exhibit this effect, because they have less plating efficiency when the current flow becomes denser. Therefore, metal plates more slowly on the outer corners than on the inner corners, resulting in a much more uniform plate thickness. Baths which produce very even plate thicknesses in this manner are described as having good throwing power. Defects such as lack of adhesion, porosity, roughness, dark spots and non-uniform coatings are likely to occur on poorly prepared parts. The surface preparation process also serves to activate the surface of the part so that it is optimally receptive to the deposition of the metal coating.²⁰

The thickness of the coated layer can be calculated using the following formulas if the coated area is known.

$$N_{i_{wt}} = 1.095 \times I \times t$$

Where:

$N_{i_{wt}}$: Weight of coated nickel [g]

I : Current [A].

t : Time of coating in second [s]

$$\text{Thicknes} = \left(\frac{Ni_{wt}}{A_{coated} \times \rho_{Ni}} \right)$$

Where:

Ni_{wt} : Weight of coated nickel [g]. ρ_{Ni} : Density of the coated nickel [g/cm³].

A_{coated} : cross sectional area of the coated layer [cm²].

Knowing that coated area is 38 cm² the thickness of the coating will be 180 μm , assuming ideal conditions with 100% anode and cathode efficiency.

Residual stress (tensile or compressive) in the nickel deposit is an important factor to control due to its tendency to cause warping or distortion of the electroformed product. Residual stress is a function of the concentration of chlorides and impurities in the plating solution. Impurities may result from breakdown of solution chemicals, trace contamination

from the anode, and drag-in from previous tanks. Stress factors near zero are obtained when chloride concentrations are as low as possible and solutions are as pure as possible.²⁰

Most engineering nickel plate applications are produced in a sulfate or sulfamate bath. Sulfamate is more commonly used because of its high plating rate and production of stress-free deposits. Alternate bath formulations may be used to yield specific properties. An example of this is the use of an all-chloride bath to achieve extremely hard, brittle deposits.²⁰

Lowenheim (1974) provided a number of different solution chemistries and discusses nickel plate applications in more detail.

The successful operation of a plating bath requires the control of at least three variables; chemical composition of the plating solution, its temperature, and the cathodic current density. These variables are related in their effect upon the character of the electrodeposits in such a way that if the range of one is changed it might not be necessary to alter the others. Since it is usually desirable in commercial production to employ maximum current densities, it is customary to adjust the bath composition, the temperature, and other factors affecting the plating operation in such a way as to attain this end. Movement of the article being plated or movement of the plating solution with respect to this article generally permits the use of higher current densities.

2.4. Experimental setup

As shown above, the electroplating cell has two electrodes, the anode, which is connected to the positive supply of the power source, is a solid pure nickel electrode, and the cathode, which is connected to the negative supply of the power source, is the 2024-T3 aluminum sample. The electroplating cell was then filled up to 19 liters with nickel sulfamate solution, which was good enough to submerge this whole assembly of anode and cathode. A continuous agitation was provided with the help of an air source inside the cell. This helps in keeping the temperature constant throughout the cell, keep the particles in continuous motion dispersed throughout the system if the particles are used, and also helps prevent any build up of debris that might hamper the coating process.

2.5. Equipment



Figure 7: Hot Plate Figure 8: Heating Element

Heating methods used to heat the solutions are as shown above in Figure 7 and 8.

In the process of precoating the first two steps (alkaline degreaser and the alkaline etch) have to be maintained at $55 \pm 5^{\circ}\text{C}$. This can be achieved by two different methods, one being the use of heating element. But the major problem that surrounds this method is the localized heating of the solution and not a good distribution of heat throughout the solution, especially around the bottom. This means that as we move away from the heating rod, the temperature drops. Also it is recommended to continuously rotate the sample inside the solution and hence not too convenient, as this will ensure proper distribution of heat and the particles throughout the bath.

In order to rectify these problems the use of hot plates was made. The hot plates used also had a provision for the stirring of the chemical solution inside. Because of the continuous stirring, the temperature was maintained throughout the chemical solution. And to add to the process, we made sure that the 2024-T3 sample was also continuously rotated. A C-PVC holder with a slight notched cut at the bottom was used to grip the sample to prevent the contamination of the substrate by hands, and also C-PVC being chemically inert, easily available and cheap.

Nickel coating is the last coating layer on the aluminum and it gives the final appearance to the part after all the cleaning and precoating process, in fact it is this layer that will have all

the mechanical, physical and chemical properties we are looking for. This process takes place in a coating cell with the following equipments.

Coating bath



Figure 9: Coating bath

The coating bath, as shown in Figure 9, was made from a non reactive material and it should be big enough to hold the coating solution, the anode, cathode, and heating element and the agitation equipments. The volume of each of the elements in the coating bath should be taken into consideration at the time of design. The volume of the coating bath tank was able to hold more than 19 liters of the chemical solution.

Heating element and temperature controller

Nickel coating are done at a temperature of 131°F ($50\pm 5^{\circ}\text{C}$). This temperature should be reached and kept stable through out coating process. This can be done though using a heating element that connects to thermal sensor. This heating element and heating controller are as shown in Figure 10 below;

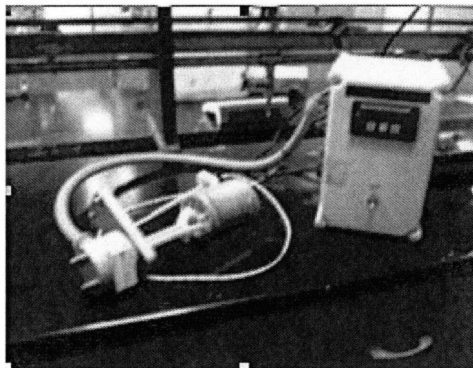


Figure 10: Heating element and heating controller for the coating bath

Power source

Current density is the main factor besides coating time in determining the thickness of the coated nickel layer, and it can be determined by the supplied current and the area of the coated sample. The current used in our experiment for coating was direct current, though pulsed current is also used, and so a converter that is capable of giving different current output, as the one shown in Figure 11, was used as a power source.

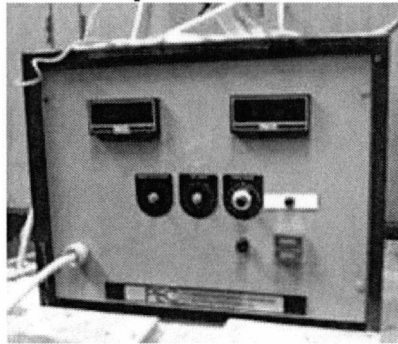


Figure 11: Power source

Miniverter was used to supply the power to the coating process. Convert alternating current to direct current. Give up to 100Amp, 50Hz.

The anode (nickel)

Nickel coating process will need a nickel source beside the nickel salt which is available from the solution. The source used was pure nickel with special feature of dissolution capabilities. This source (the anode) was covered by a special cover (bag) that let nickel ion go to the solution and prevent any oxides or impurities from moving to the solution. Nickel anode and anode bag are both shown below in Figure 12 and 13 respectively.



Figure 12: Nickel anode

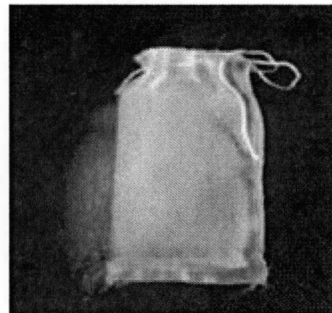


Figure 13: Anode bag

Cathode holder

The sample needs to be held upright parallel to the anode positioned away from the tank wall; also it must be kept under the solution all the time in a fixed position. That was achieved by using a special holder. The holder material should not be conductive. If it is conductive it will be coated with nickel and then current density calculation will be away from reality. The existence of a non conductive material in touch to the sample will disturb the current field around the sample, and that will affect the coated layer. So it will be better to have the grip made of copper or any other conductive material and the holder from PVC. The cathode holder is as shown in the Figure 14 below;

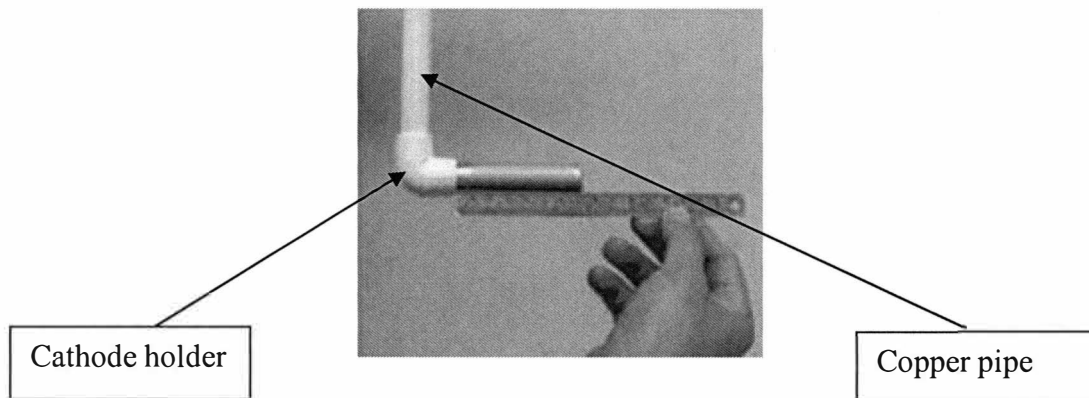


Figure 14: Cathode holder

Agitator and air filter

Since a non-soluble nano particles were used in this coating an agitation process had to be used in the coating tank. Agitation is also necessary to remove any agglomeration of particles around each other or over the sample it self. Such agglomeration around the sample will block the nickel particles from reaching the sample surface. The best way to have the agitation is by using a stream of controlled-flow- filtered air. The air flow meter and controller with the bubbulator are shown below in Figures 15 and 16.

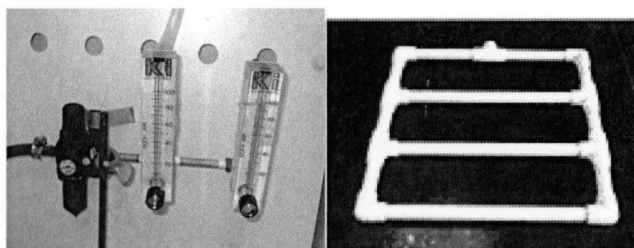


Figure 15: Air flow meter and controller

Figure 16: Bubbulator

2.6. Chemicals

Chemicals that were chosen for this set of experiment are specifically designed to be used for the aluminum alloys. The precoating assembly consisting of the alkaline degreaser, alkaline etch, acidic etch, and zincate is arranged as shown below in Figure 17.

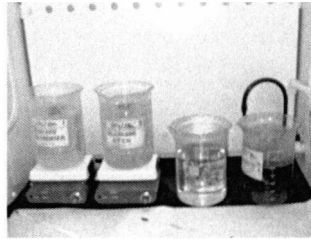


Figure 17: Precoating assembly

Alkaline Degreaser

As already mentioned earlier Disodium Trioxosilicate solution is used as alkaline degreaser in order to clean the sample surface. To get a better cleaning the solution should be heated to $55\pm 5^{\circ}\text{C}$. The cleaning of the substrate surface is done by changing chemical nature of the dirt, or the grease from insoluble to soluble materials by displacing the hydrophobic group by a hydrophilic group, which in turn allows the grease to leave the sample surface and into the solution by a process similar to saponification. The time required for this process depends on the amount of machining that the sample went through, or the amount of debris on the sample surface, but in our process we kept it to 8 minutes, which was good enough considering it was a thin sheet.

Alkaline Etching

The alkaline etching is done by a solution of sodium hydroxide. The reaction was done at 55 ± 5 °C and for a period of 3 minutes.

Acidic Etch

The third step involves the use of Nitric (HNO_3) with Hydrochloric (HCl) acids 25% each in de-ionized distilled water balance 50%. It is done twice. The main purpose of this stage is to remove the product of alkaline etching in order to prepare the surface for zincating and later to remove the thick and porous zincate layer.

Zincate

A solution of zincate ZnSO_4 is used in this stage. By the immersion of the sample in this solution, the sample will be covered with a thick layer of zincate, which will be non uniform and porous. This layer is dissolved in acidic media, and when repeated, gives a second layer which is thinner and uniform. Zincate layer is the base for nickel, since nickel cannot adhere to aluminum.

Nickel sulfamate ($\text{Ni}(\text{NH}_2\text{SO}_3)_2$)

Nickel sulfamate is an electrolytic solution that will provide the media for coating and allow nickel ions to move from the anode to the cathode. The pH of this solution must be kept constant through coating process and that is done by measuring the pH at the operating condition every time we move from one step to another. The pH of the solution will drop down to be more acidic as the coating process is progressed. To bring the pH back to its original value a pH adjustor must be added to the solution, the nature of that adjustor will be discussed a later.

Sodium Cobaltinitrite

Sodium cobaltinitrite $\text{Na}_3\text{Co}(\text{NO}_2)_6$ was used as an electroplating additive for depositing nickel with nano-sized SiC particles. “This additive promotes the co-deposition of SiC particles.”²¹

Various types of bath, as shown in the Table 3 below, have been used for nickel. The throwing power has been one of the main drawbacks of these solutions. Given below, in Table 3, is the comparison of various kinds of baths that have been used.

Table 3: High throwing power nickel electroplating and its application²²

Bath Type	Ni (g/L) in bath	Throwing Power (%)
Watts type bath	73	6
Low Ni Watts type	12	6
Ni Sulfamate bath	73	8
Ni chelated bath	24	-11
High T.P. sulfate bath	12	30
High T.P. Halide bath	12	50
Bath pH	4.4	
Bath temperature	55 deg C	
Cathode current density	1 A/dm²	
Agitation	Cathode rocking, 1m/min	

Bath	Hardness (Hv)	Stress (Kg/mm ²)	Ductility (mm)
Watts type	241	42	5
Ni sulfamate	280	-7	6
High T.P. sulfate	213	16	8
High T.P. halide	278	44	6

As seen from the above comparison sheets, we decipher that using nickel sulfamate bath is a good choice.

pH adjustor

The pH of the coating solution will affect the way the coating proceeds on the aluminum substrate. If the pH is too high (more basic) the coating will not adhere to the surface. On the other hand if the pH is too low (more acidic), the coated layer will comprise of coarse grain structure with a high level of residual stresses. We tried to keep the pH of the bath around 4.4 – 4.5.²²

Use of crystalline sodium hydroxide (washing soda) which has a pH of 11 for a saturated solution was made to adjust the pH of the coating bath which was later switched to sodium hydroxide; the addition of sodium hydroxide was done slowly and gradually over a long period of time in order to ensure that the agglomeration of the particles does not take place and it is distributed evenly throughout the solution.

Silicon Carbide (SiC)

Nano silicon carbide particles were incorporated into the nickel metallic matrix, and the comparison was made of the coatings with and without the nano silicon carbide particles.

2.7. Residual stress hole drilling²³

2.7.1. Procedure

Briefly summarized below, the measurement procedure involves six basic steps:

1. A special three-element strain gage rosette is installed on the test part at the point where residual stresses are to be determined.
2. The three gage grids are wired and connected to a static strain indicator through a switch and balance unit.
3. A precision milling guide is attached to the test part and accurately centered over a drilling target on the rosette.
4. After the zero balancing of the gage circuits, a small, shallow hole is drilled through the center of the rosette.
5. Readings are made of the relaxed strains, corresponding to the initial residual stress.
6. Using the special data-reduction relationships, as standardized in ASTM standard test method E837, the principal residual stresses and their angular orientation are calculated from the measured strains.

2.7.2. Installation of the strain gage

The initial step in preparing for any strain gage installation is the selection of the appropriate gage for the task. Careful, rational selection of gage characteristics and parameters can be very important in optimizing the gage performance for specified environmental and operating conditions, obtaining accurate and reliable strain measurements, contributing to the ease of installation, and minimizing the total cost of the gage installation. CEA-XX-062UL-120 special rosette strain gage as shown in Figure 18 was chosen for our experiments, and its specifications are shown in Table 4.

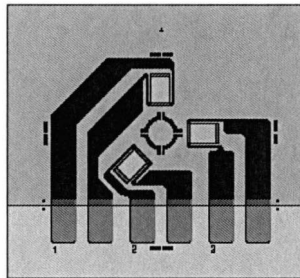


Figure 18: CEA-XX-062UL-120 special rosette strain gage

2.7.3. Specifications

Different strain gage rosettes have different specifications, according to their properties and also the desired results. It might include the ease of fabrication and soldering too.

Table 4: Specifications of the CEA-XX-062UL-120 strain gage rosette

Dimensions	inch	mm
Gage length	0.062	1.57
Grid centerline diameter	0.202	5.13
Typical hole diameter (min)	0.06	1.5
Typical hole diameter (max)	0.08	2.0
Matrix length	0.50	12.7
Matrix width	0.62	15.7

Resistance in ohms: $120 \pm 0.4\%$

This special strain gage rosette is fully encapsulated with large copper-coated soldering tabs. Installation time and expense are greatly reduced and all solder tabs are on one side of the gage to simplify lead wire routing from the gage site.

The purpose of the surface preparation is to develop a chemically clean surface having a roughness appropriate to the gage installation requirements and visible gage layout lines for locating and orienting the strain gage.

Four basic operations of surface preparation for aluminum alloys are as follow;

1. Solvent degreasing

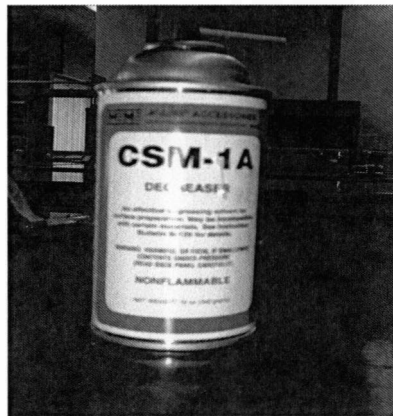


Figure 19: Degreaser

The main application here was to clean the surface of the sample from any impurities, which was done by CSM-1A, as shown in Figure 19. The surface was kept clean and wet with the use of the conditioner and is applied by a sponge from centre of the sample to the outside.

2. Application of gage layout lines

This was done in order to get the rosette exactly at the place where we wanted to study the residual stresses. This was achieved by using a 4H pencil, so that the marks made by the same were visible even after it is cleaned with cotton swabs later.

3. Neutralizing

This was done to provide optimum alkalinity for the strain gage adhesives to be used later. Neutralizer 5A was used for the same purpose. This was applied on the surface for 1 minute and was cleaned off with a clean sponge.

4. Rosette Bonding

This was achieved in several stages as described below;

1. The strain gage was removed from its acetate envelope by grasping the edge of the gage with tweezers, and was placed on a chemically clean glass plate, with the shining surface looking up.
2. A small terminal was attached to the gage, so that if the wire is taken off during the process, the gage is not disturbed. This was placed at a distance of 2-3 mm from the gage.
3. The gage with the terminal was then covered with a clean cellophane tape. The tape was firmly wiped down over the gage and the terminal.
4. The tape was then taken off, at a shallow angle of not more than 30 degrees so that the gage and the terminal come off with it.

5. The tape was then placed carefully over the grid lines previously marked on the sample, so that the center of the gage was at the point of study.
6. The tape was then folded backward leaving 2-3 mm between the terminal and the substrate. Whole gage area was then brushed with Catalyst-C, and was left for 1 minute.
7. Two to three drops of the adhesive were then applied at the bottom of the tape, and then the tape was put back on the sample. This was pressed tightly for a couple of minutes.
8. The tape was then taken off at a much steep angle close to 60 degrees, in order to keep the gage and the terminal on the sample.
9. Wires were then soldered on the terminal and from the terminal to the gage. Conducting tape was put over the wire during the solder to keep it in place, and also to keep the strain gage in place. A thin coat of M coat A, as shown in Figure 20, was applied over the strain gage and the terminal to preserve the coating for a long time.



Figure 20: Adhesive kit and preserve coat

Figures 21-26 show the main process of hole drilling, starting with the gage assembly, the hole drilling setup, the gage assembly in the hole drilling setup, switch balance units and the drilled hole.

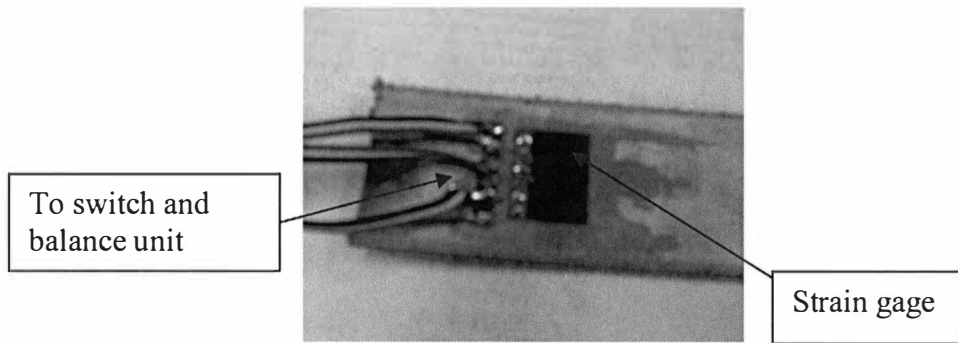


Figure 21: Gage assembly

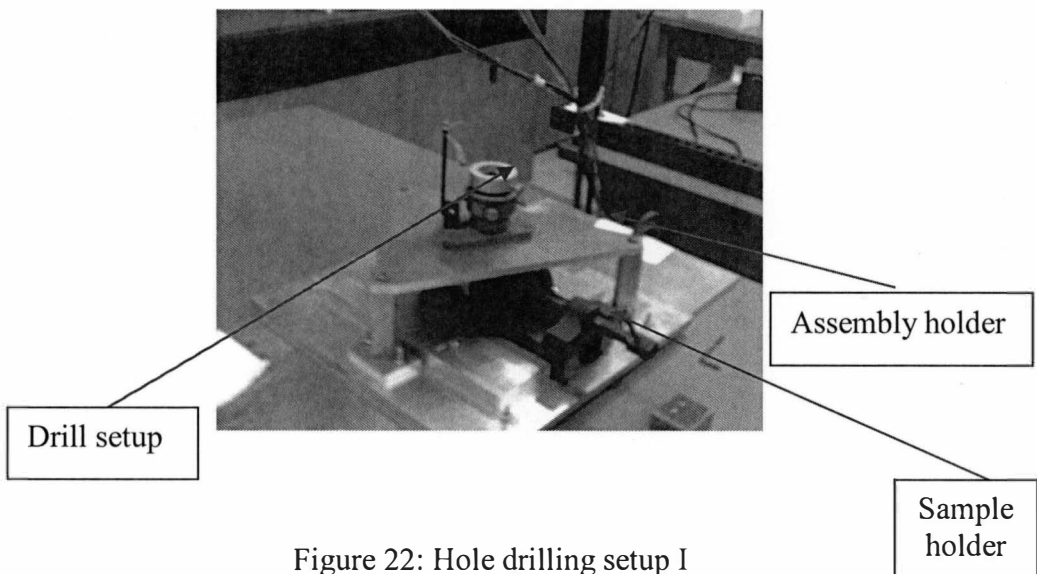
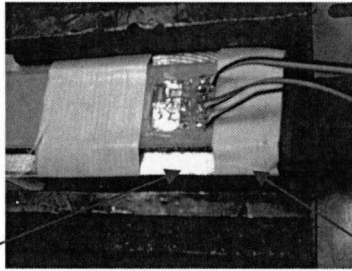


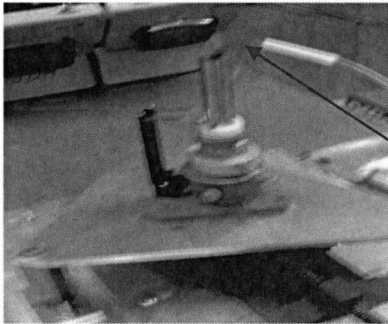
Figure 22: Hole drilling setup I



Strain gage

Figure 23: Gage assembly in the setup

Soldered wires



Drill

Figure 24: Hole drilling setup II



Figure 25. Switch balance units

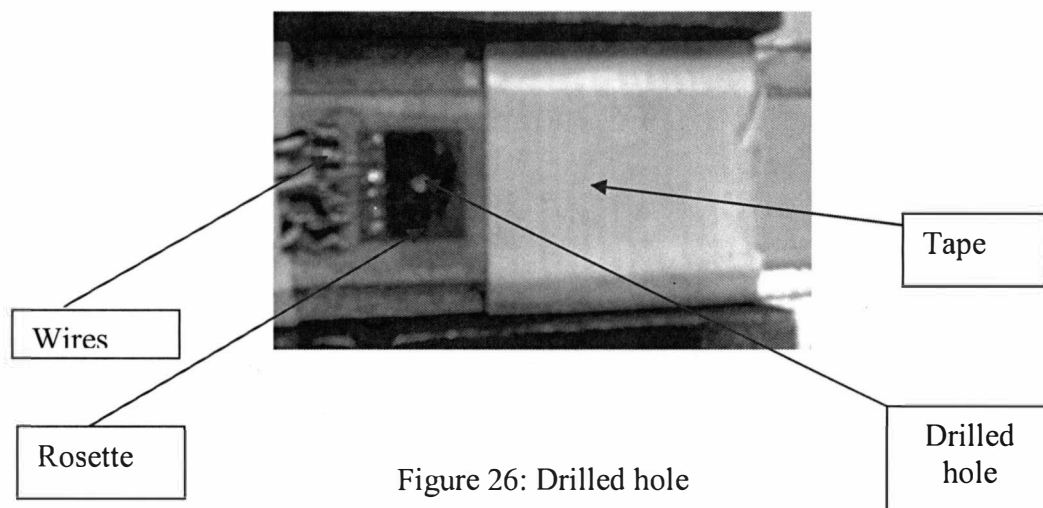


Figure 26: Drilled hole

The solder wired were then connected to the switch balance units, and the setup was ready to take the readings. These were given in terms of strains as ϵ_1 , ϵ_2 or ϵ_3 depending on the unit we were using, and they were numbered 1 -3 left to right.

The equivalent uniform principal stresses and their directions were then calculated at each increment, using the equations below;

$$\sigma_{\max/\min} = (\epsilon_1 + \epsilon_3)/4A \pm \{[(\epsilon_3 - \epsilon_1)^2 + (\epsilon_3 + \epsilon_1 - 2\epsilon_2)^2]^{0.5}\}/4B \text{----- (equation 1)}$$

$$\tan 2\alpha = [\epsilon_1 - 2\epsilon_2 + \epsilon_3]/[\epsilon_3 - \epsilon_1] \text{----- (equation 2)}$$

2.8. Evaluation of stress in metallic films deposited by electrolysis using the bending method²⁴

The thickness of the substrate we have is extremely small, i.e. 0.06 mm, and hence there is some bending in the final coated sample as that is shown in Figure 27 below. The amount of bending is coupled with this thickness. The stress in the metallic films deposited by electrolysis is calculated by the following formula;

$$P = 4/3 (Ed^2z/tl^2)$$

Where;

E = Young's modulus of nickel (Kg/cm²)

d = thickness of sample substrate (cm)

z = deflection of the sample from neutral axis (cm)

t = thickness of the coating (cm)

l = length of the sample substrate (cm)

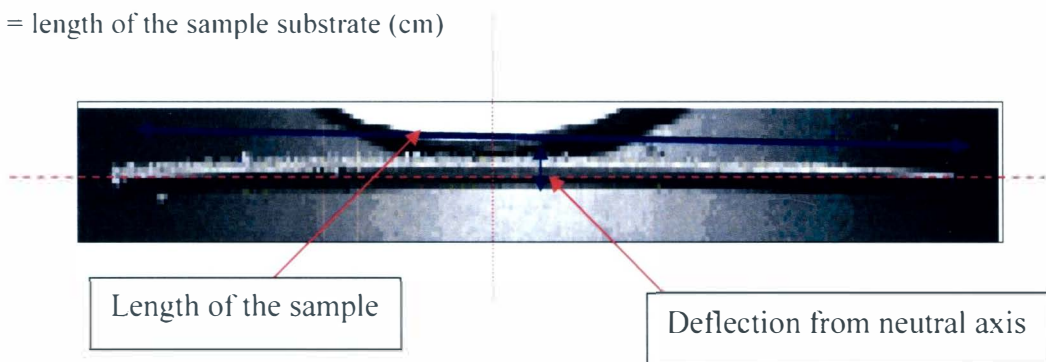


Figure 27: Coated sample showing the bending

2.9. Corrosion (potentiodynamic) setup

Potentiodynamic study were carried out in the corrosion setup as shown;

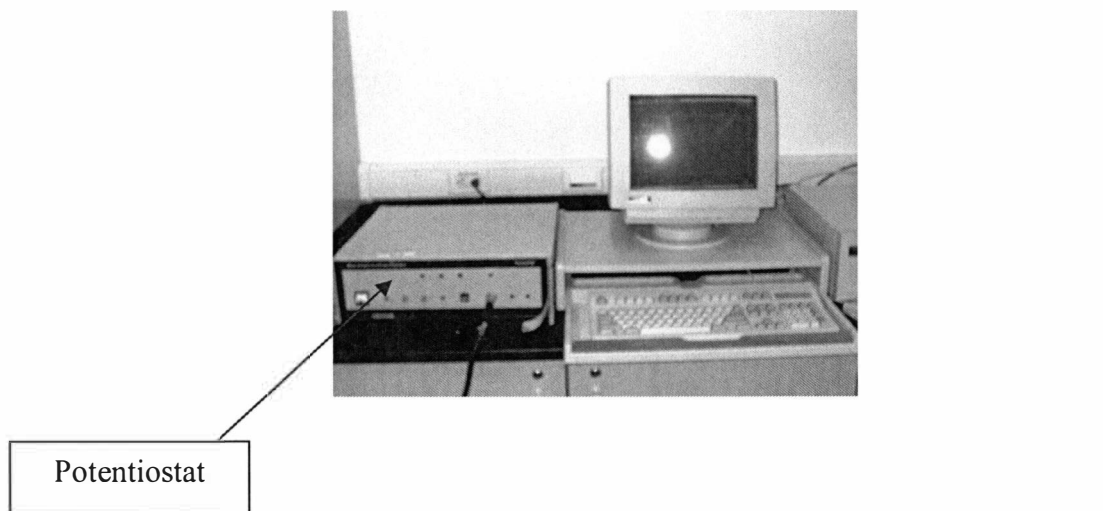


Figure 28: Potentiodynamic setup

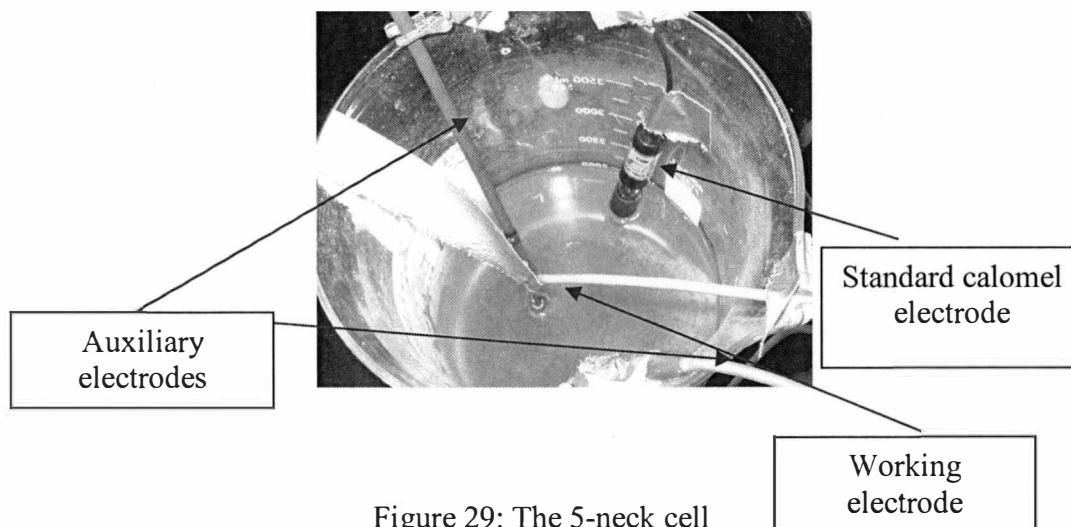


Figure 29: The 5-neck cell

The basic setup consisted of an EG&G Princeton potentiostat, connected to a personal computer, which in turn was connected to the printer, as shown in Figure 28. The software used was corr352, which is corrosion software. The potentiostat was connected to a 4 liter beaker which contains two auxiliary electrodes, a standard calomel reference electrode, and the sample to be studied, as shown in Figure 29.²⁵⁻²⁸

The parameters are fed in to the software program and then kept constant throughout the experiment.

2.9.1. Run parameters²⁶⁻²⁸

1. Initial E (mV): This represents the lower limit of the scan potential, i.e. in the cathodic region with respect to the free corrosion potential.
2. Final E (mV): This represents the upper limit of the scan potential, i.e. in the anodic region with respect to the free corrosion potential.
3. Scan rate (mV/second): The scan rate determine the rate of the change of potential. The total time required for the experiment depends on the scan rate. The scan-rate chosen was not too high otherwise considerable deviation from the linearity will be obtained; as the specimen is not allowed sufficient time to react with the applied potential. The initial delay should be at least one minute. If the initial delay is not provided the scan starts immediately on removal of the conditioning potential, this results in the fluctuations in the curve.

2.9.2. Sample parameters²⁶⁻²⁸

1. Area of the specimen (cm²)
2. Equivalent weight (gms)

$$(\text{Equivalent weight} = \text{atomic weight/valency})^{29}$$

3. Density (gm/cm³)
4. Condition potential (mV)
5. Condition time (sec)

The plot between the potential and log current density/ current density is obtained, and then comparative study of the various samples in the same corrosive environments is made.

Potentiodynamic output from the corr352 software is shown below in Figure 30.

```

Model 352/252 Corrosion Analysis Software, v. 2.18
Filename: c:\352\data\amit ni
Pstat: UStatII Ver 2
PD POTENTIODYNAMIC
Date Run: 89-09-02
File Status: NORMAL
Time Run: 19:43:47

Conc. Time CT 60 s
Conc. Pot. CP -1.000 V
Initial Delay ID 180 s
Scan Rate SR 2.000 mV/s
Scan Incr. SI 1.000 mV
No. of Points NP 1447
Curr. Range CR Auto
Step Time ST 500.0E-3 s
GI Time Const. TC Off
IR Mode IR none
Filter FL Off
Working Elec. WE Solid
Ref. Elec. RE SCE 241.5E-3V
Sample Area SA 5.000 cm2
Density DE 8.898 g/ml
Equiv. Wt. EW 35.00 s
Open Circuit OC 3.188 V
AUX A/D AU no

Comment: Nickel 0.6M NaCl
----- amit ni

```

Figure 30: Potentiodynamic output

2.10. Tensile tests²⁹

The tensile tests were carried on using a setup as shown in Figure 31. It consisted of a strain indicator as an optional attachment to give the values of load per unit area even at lower values of the strain.

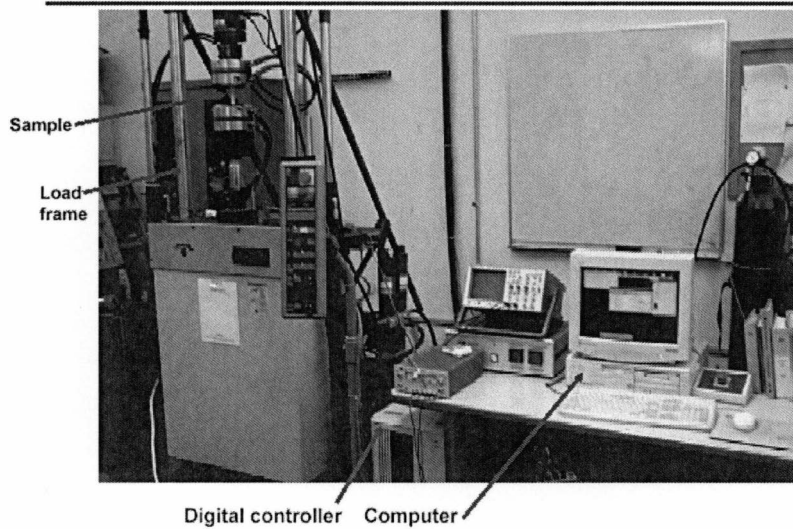


Figure 31: Tensile test setup

2.11. Wear tests

The apparatus used, Pin-on-reciprocating-plate tribometer (courtesy Seiyed Mirmiran, Autoshellcraft Daimler Chrysler), had the following specifications:

1. Top ring facing

Normal composition 75% molybdenum, 25% nickel chrome, boron, and silicon.

Hardness – 950-1050 Vickers with 50 gm load

(Molybdenum interstitially hardened with boron)

2. Top ring material

Martensitic nodular iron hardness to RC 25.

3. Cylinder bore material

Induction hardened gray iron with a surface hardness of RC 40 minimal.

(Induction hardening produces a martensitic structure)

4. Properties of materials

4.1 Top ring – Modulus of elasticity is 3480 MPa (24,000,000 PSI)

- Transverse rupture strength is 14.5 MPa (100,000 PSI)

4.2 Cylinder bore base material class 35 gray iron

- Modulus of elasticity is 1740 MPa (12,000,000 PSI)

- Strength is 5 MPa (35,000 PSI) minimum

2.12. Samples and the coating parameters

2.12.1. Tensile samples

Sample (Coating)	Current (Amp)	Coating Time (Min)	Agitation (m ³ /h) (SCFH)
Aluminum Only	18	28	2.83 (100)
Al Nickel Only	18	28	2.83 (100)
Al Nickel SiC 7g/L	18	28	2.83 (100)
Al Nickel SiC 21g/L	18	28	2.83 (100)
Al Nickel SiC 42 g/L	18	28	2.83 (100)

$$\text{Current Density} = 0.72 \text{ A/cm}^2$$

2.12.2. Rectangular samples

Sample (Coating)	Current (Amp)	Coating Time (Min)	Agitation (m ³ /h) (SCFH)
Aluminum Only	18	28	2.83 (100)
Al Nickel Only	18	28	2.83 (100)
Al Nickel SiC 7g/L	18	28	2.83 (100)
Al Nickel SiC 21g/L	18	28	2.83 (100)
Al Nickel SiC 42 g/L	18	28	2.83 (100)

CHAPTER III

EXPERIMENTAL RESULTS

3.1. Dimensions of tensile specimens

Given below in Table 5 are different tensile specimens that were tested for stiffness. We tested five different samples that were bare aluminum, aluminum with nickel coating, and aluminum with different amount of nano silicon carbide in the coating bath. Given below in table 5 are the thicknesses of aluminum substrate and the total thickness of the sample after the coating. The thickness was calculated using scanning electron microscope.

Table 5: Dimensions of the tensile specimens

Sample (Coating)	Thickness of the aluminum measured by SEM μm^{30}	Total thickness of the sample μm^{30}
Aluminum	632	632
Al – Ni only	593	643
Al – Ni – 7 g/L SiC	575	639
Al – Ni – 21 g/L SiC	546	611
Al – Ni – 42 g/L SiC	583	648

3.2. Residual stress results

3.2.1. Hole drilling

Given below in Table 6 are the values of the measured strains and the relieved strains. They were obtained from the switch and balance unit after each increment of the depth. They were taken directly from the instrument and were recorded as given below. We went to 200 microns of the coating depth.

Table 6: Measured strains and relieved strains

Depth		Measured Strain			Relieved Strains		
Z in (cm)	Z/D	ϵ_1	ϵ_2	ϵ_3	$\epsilon_3 + \epsilon_1$	$\epsilon_3 - \epsilon_1$	$\epsilon_3 + \epsilon_1 - 2 \epsilon_2$
0 (0)	0	0	0	0	0	0	0
0.001 (0.0025)	0.00495	8	6	-3	5	-11	-7
0.002 (0.005)	0.009901	-4	-7	-9	-13	-5	1
0.003 (0.075)	0.014851	-4	-8	-9	-13	-5	3
0.004 (0.01)	0.019802	-6	-10	-11	-17	-5	3
0.005 (0.0125)	0.024752	-9	-13	-12	-21	-3	5
0.006 (0.015)	0.029703	-16	-20	-15	-31	1	9
0.007 (0.0175)	0.034653	-14	-17	-15	-29	-1	5
0.008 (0.02)	0.039604	-12	-16	-14	-26	-2	6

Given below in Table 7 are the values of the coefficients calculated using ASTM E837. These values are obtained from the relieved strains, as given in the Table 5.2.1., and are applied in the final formula used for the calculations of the minimum and the maximum residual stresses.

Table 7: Calculated values of coefficients

Coefficients					
a	b	A	B	4A	4B
0	0	0	0	0	0
0	0	0	0	0	0
0.005	0.01	-1.09E-10	-1.66667E-10	-4.36E-10	-6.66667E-10
0.01	0.02	-2.18E-10	-3.33333E-10	-8.72E-10	-1.33333E-09
0.012	0.03	-2.62E-10	-5E-10	-1.05E-09	-0.000000002
0.016	0.035	-3.49E-10	-5.83333E-10	-1.4E-09	-2.33333E-09
0.02	0.04	-4.36E-10	-6.66667E-10	-1.74E-09	-2.66667E-09
0.025	0.05	-5.45E-10	-8.33333E-10	-2.18E-09	-3.33333E-09
0.03	0.055	-6.54E-10	-9.16667E-10	-2.62E-09	-3.66667E-09

Table 8 gives the value of the obtained stress from the calculations in psi and then in MPa. The Table also gives the values of the angles at which these stresses are present.

Table 8: Measured residual stresses and their orientation

Uniform Stress to Depth Z		Uniform Stress to Depth Z (1000 psi)		Uniform stress to depth Z (MPa)	
σ min	σ max	σ min	σ max	σ min	σ max
2216798449					
1	37465043032	22.17	37.47	152.85	258.32
1053504296					
0	19281470802	10.54	19.28	72.64	132.95
1333070142					
3	19161653317	13.33	19.16	91.92	132.12
1255262612					
1	17550584888	12.55	17.55	86.55	121.01
1437945993					
1	21170998785	14.38	21.17	99.15	145.97
1177304644					
0	14832458148	11.77	14.83	81.18	102.27
8213959197	11663716644	8.21	11.66	56.64	80.42
Uniform stress to depth Z (MPa)					
σ min		σ max		$\tan 2 \alpha$	α
				0	0
				-7	-40.9
152.85		258.32		1	22.5
72.64		132.95		3	35.78
91.92		132.12		3	35.78
86.55		121.01		5	39.35
99.15		145.97		9	41.83
81.18		102.27		5	39.35
56.64		80.42		6	40.27

α is measured taking the center of the vertical axis of the sample as zero

3.2.2. Bending due to tension

The amount of the bending, with the thickness of the deposit made it possible for us to calculate the tension under which the coating was deposited. The following formula was used to calculate the tension per unit area of the section on the nickel film

$$P = 4/3 (Ed^2z)/tl^2$$

Where;

Young's modulus of nickel (E) = 2,100, 000 kg/cm² (206 GPa)

Thickness of the aluminum sheet (d) = 0.06 cm

Deflection of the this sheet of the coated sample (z) = 0.6 cm

Thickness of the nickel coating (t) = 0.02 cm

Total length of the coated sample (l) = 13.8 cm

Calculated with the above formula we got the value of the tension = 155 MPa

3.3. Corrosion tests (potentiodynamic)

Shown in Figure 32 is the corr352 output for bare aluminum in 0.6M NaCl. The output also shows the fixed run parameters and the sample parameters. The Figure clearly shows a tendency of aluminum to corrode rather fast and later going into passivation. The passive nature of the aluminum can be explained by the formation of a thin film of reactant

products over the sample. Because of the presence of this film, the aluminum ceases to corrode and goes into passivation.

```

Model 352/252 Corrosion Analysis Software, v. 2.10
Filename:
Pstat: VStaff1 Ver 2
PD POTENTIODYNAMIC
Date Run: 09-29-82
File Status: EDITED
Time Run: 18:30:58

Cond. Time CT 60 s Initial Pot. IP -250.0E-3 V
Cond. Pot. CP -1.000 V Final Pot. FP 1.000 V
Initial Delay ID 100 s

Scan Rate SR 2.000 mV/s Curr. Range CR Auto
Scan Incr. SI 1.000 mV Step Time ST 500.0E-3 s
No. of Points NP 1851

Line Sync. LS no
Rise Time RT high stability
Working Elec. WE Solid
Sample Area AR 7.500 cm2 Ref. Elec. RE SCE 241.5E-3V
Density DE 2.285 g/ml AUX A/D AU no
Open Circuit OC 2.720 V

Comment: aluminum 06M NaCl
  
```

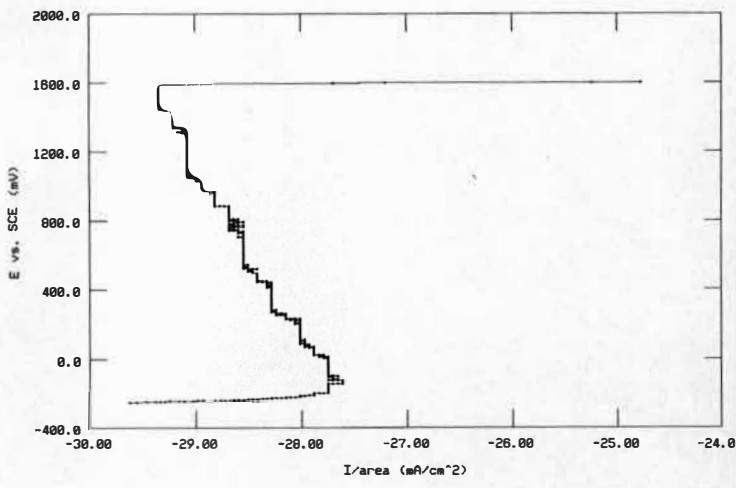


Figure 32: Aluminum in 0.6 M NaCl

Figure 33 shows the corr352 output for the sample of aluminum-50 micron nickel coating. It can be seen from the plot that the composite sample corrodes at lower potentials and then goes into passivation which results in a vertical line, showing the increase of the potential at a constant current density.

Model 352/252 Corrosion Analysis Software, v. 2.10
 Filename: c:\m352\data\amit ni
 Pstat: UStaff() Ver 2
 PD POTENTIODYNAMIC
 Date Run: 09-29-82
 File Status: NORMAL
 Time Run: 19:43:47

Cond. Time	CT	60	s	Initial Pot.	IP	-250.0E-3	V
Cond. Pot.	CP	-1.000	V	Final Pot.	FP	1.600	V
Initial Delay	ID	180	s				
Scan Rate	SR	2.000	mV/s	Curr. Range	CR	Auto	
Scan Incr.	SI	1.000	mV	Step Time	ST	500.0E-3	s
No. of Points	NP	1447					
Line Sync.	LS	no		GI Time Const.	TC	Off	
Rise Time	RT	high stability		IR Mode	IR	none	
Working Elec.	WE	Solid		Filter	FL	Off	
Sample Area	AR	5.000	cm ²	Ref. Elec.	RE	SCE 241.5E-3V	
Density	DE	8.890	g/ml	Equiv. Wt.	EW	35.00	g
Open Circuit	OC	3.160	V	AUX A/D	AU	no	

Comment: Nickel 0.6M NaCl

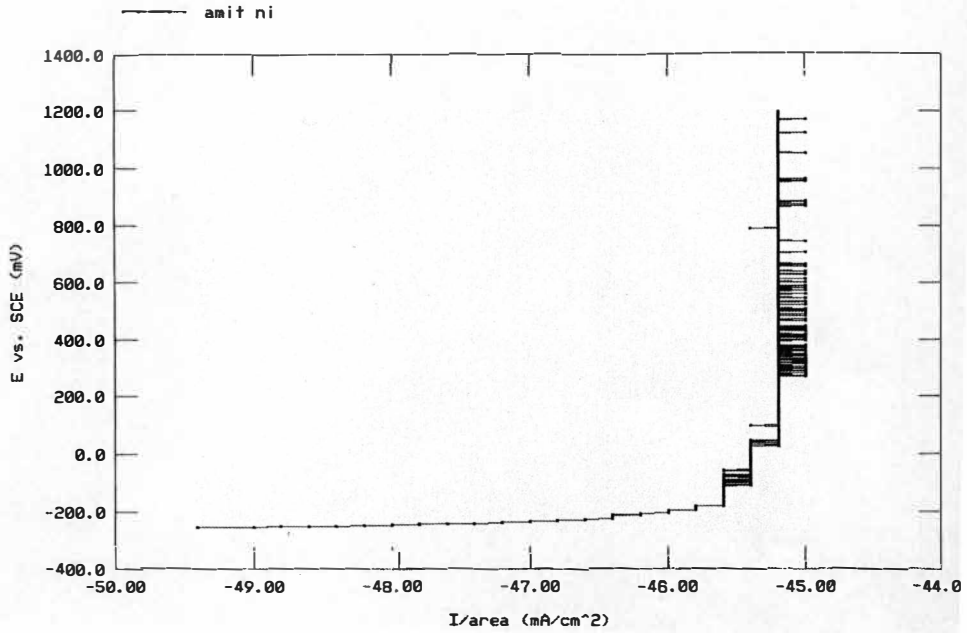


Figure 33: Nickel 50 microns in 0.6 M NaCl

Figure 34 shows the output for aluminum with 208 microns nickel coating. Interesting here is that unlike the 50 micron nickel coating, this curve shows a tendency to go into the trans-passive region of the plot. This result in a higher value of the corrosion rate, as when compared to the 50 micron nickel coating.

Model 352/252 Corrosion Analysis Software, v. 2.10

Filename: c:\m352\data\amit 200

Pstat: VStat[] Ver 2

PD POTENTIODYNAMIC
Date Run: 09-29-82

File Status: NORMAL
Time Run: 20:13:13

Cond. Time	CT	60	s	Initial Pot.	IP	-250.0E-3	V
Cond. Pot.	CP	-1.000	V	Final Pot.	FP	1.600	V
Initial Delay	ID	100	s				
Scan Rate	SR	2.000	mV/s	Curr. Range	CR	Auto	
Scan Incr.	SI	1.000	mV	Step Time	ST	500.0E-3	s
No. of Points	NP	1333					
Line Sync.	LS	no		GI Time Const.	TC	Off	
Rise Time	RT	high stability		IR Mode	IR	none	
Working Elec.	WE	Solid		Filter	FL	Off	
Sample Area	AR	5.000	cm ²	Ref. Elec.	RE	SCE 241.5E-3V	
Density	DE	8.890	g/ml	Equip. Wt.	EW	35.00	g
Open Circuit	OC	2.800	V	AUX A/D	AU	no	

Comment: Nickel 0.6M NaCl

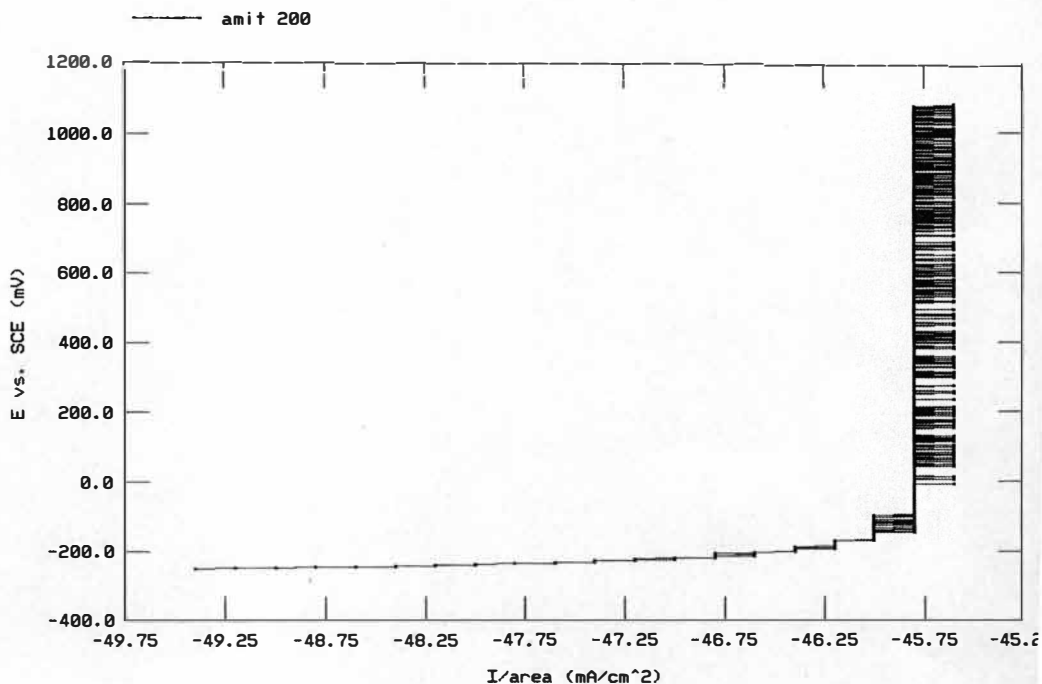


Figure 34: Nickel 208 microns in 0.6 M NaCl

Table 9 summarizes the results obtained from the corr352 software, in terms of corrosion rate. It is evident that the values for E_{corr} are highest for bare aluminum and are lowest for the aluminum-208 micron nickel sample. This indicates least corrosion rate for the 208 micron nickel sample. But the corrosion rate as obtained from the software is not in agreement with the E_{corr} values. According to these values, the 50 micron nickel sample has

the least corrosion rate. This is due to the fact that the 208 micron corrosion sample, due to its thickness, already had pitting sites, that initiated the pitting corrosion rather early.

Table 9: Corrosion rate values for the samples

Sample	Corrosion Rate (mmpy)	E _{corr} (volts)	I _{corr} ($\mu\text{A}/\text{cm}^2$)	Tafel's Constant (v/d) Ba & Bc
Aluminum	7.815	3.713	156.1	100E-3
Ni 50 μm	6.099	2.109	474.0	100E-3
NI 208 μm	7.594	1.678	590.2	100E-3

3.4. Tensile tests

Tensile test plots for the samples are given below in Figure 35, and the calculated values are given in Table 10. The plots clearly show that the slope gets steeper as we go from bare aluminum to aluminum-Ni-42 g/L SiC sample. This is not surprising, considering, that the Young's modulus of nickel is 3 times and that of silicon carbide is 6 times that of aluminum. Therefore, as we increase the amount of silicon carbide in the coating bath, the stiffness also increases.

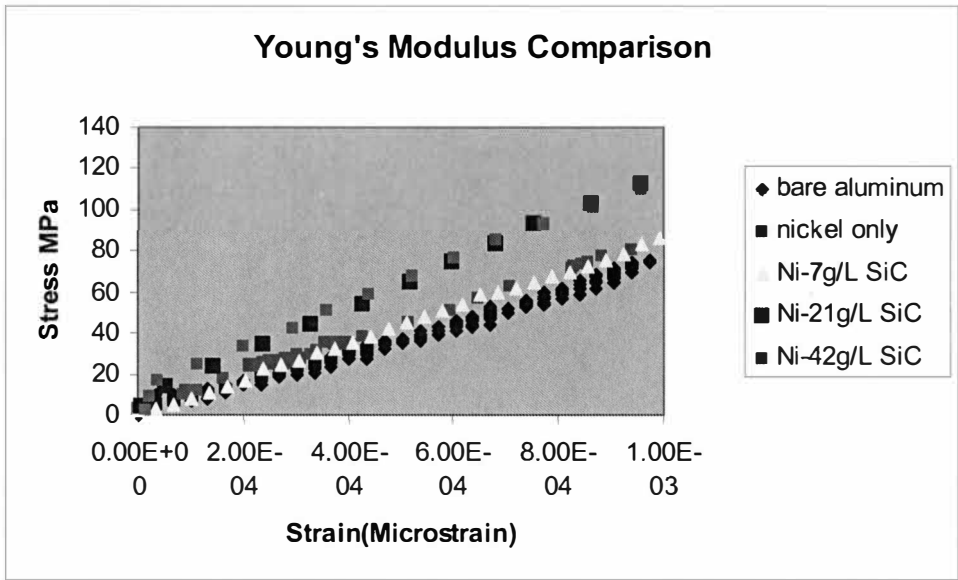


Figure 35: Elastic zone comparison for the samples

Table 10: Combined table for Young's modulus

Sample	E from plots GPa	Thickness of coating, mm Taken from SEM ³⁰	Total Thickness, mm	Thickness of Al, mm	E of coating, GPa
Al	72	0	0.632	0.632	NA
Ni Only	82	0.05	0.643	0.593	199
7 g/l	86	0.064	0.639	0.575	207
21 g/l	112	0.065	0.611	0.546	444
42 g/l	109	0.065	0.648	0.583	432

3.5. Wear test results

Table 11: Nickel – 7g/L SiC coated sample

Sample	Aluminum-Ni-SiC sample
Pre-wear weight (g)	1.1776
Normal Force applied (N)	5.1
WC ball diameter (∞m)	1389
Weight prior to wear	1.1776 grams
Total Wear Test Duration	~ 11minutes
Motor RPM	varied
Total number of cycles	~1280
Travel distance / cycle	19mm
Total distance traveled	48.64 m
traverse speed	varied
Strain readout sensitivity	1 µstrain per mV output
Calibration rate	~24 mN/microstrain
Frictional Force	varied
Final Wear Width	376 µm
Final Wear Depth	13 µm
Density (mg/mm³)	11.5

Table 11—continued

Speed (RPM)	Duration (min)	Strain (μs)	Post-Wear Weight (g)	Wear Loss (g) for each step
25	4	170	1.1776	0.0000
60	2	125	1.1776	0.0000
100	2	60	1.1775	0.0001
200	1	22	1.1774	0.0001
300	1	16	1.1772	0.0002
360	1	7	1.1769	0.0003

Wear Loss (g) accumulative	Speed (mm/s)	Friction Force (mN)	Coefficient of friction	Wear Depth (μm)	Wear Width (μm)	accum Wear Vol. (mm^3)
0.0000	16	4103	0.80	0	0	0.000
0.0000	38	3017	0.59	0	0	0.000
0.0001	63	1448	0.28	3	197	0.009
0.0002	127	531	0.10	6	248	0.017
0.0004	190	386	0.08	9	312	0.035
0.0007	228	169	0.03	13	376	0.061
Total number of cycles			1280			
Total Traveled Distance (m)			48.64			
Total Wear Mass Loss (g)			0.0007			

Figure 36 shows the friction force vs. sliding speed plot for Ni-7g/L SiC sample as obtained from the wear test. It is clearly evident from the plot that as the sliding speed is increased, the friction force required decreases.

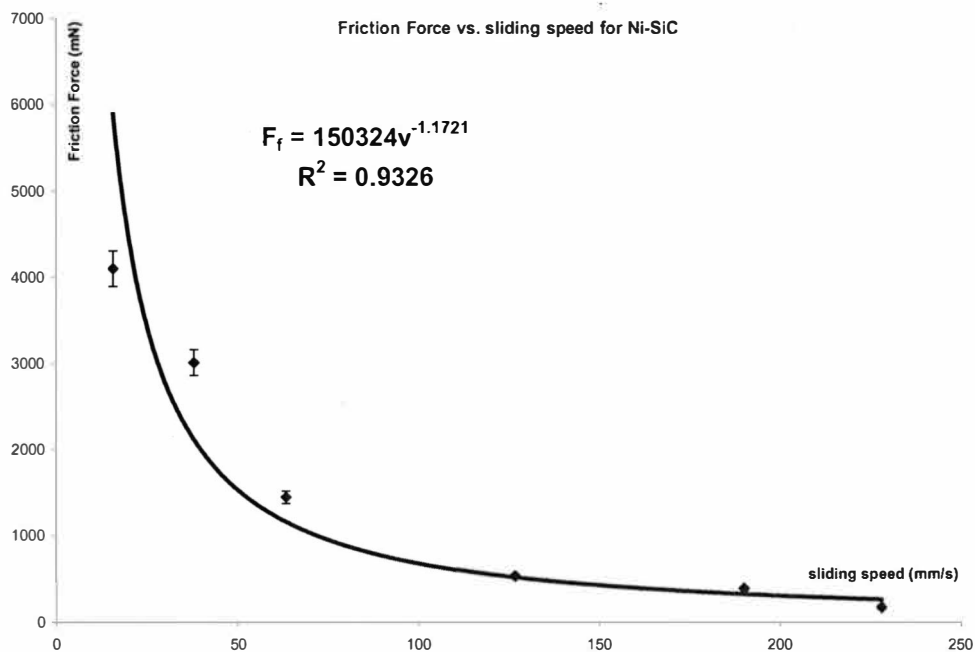


Figure 36: Friction force vs. sliding speed plot for Ni-7 g/L SiC sample

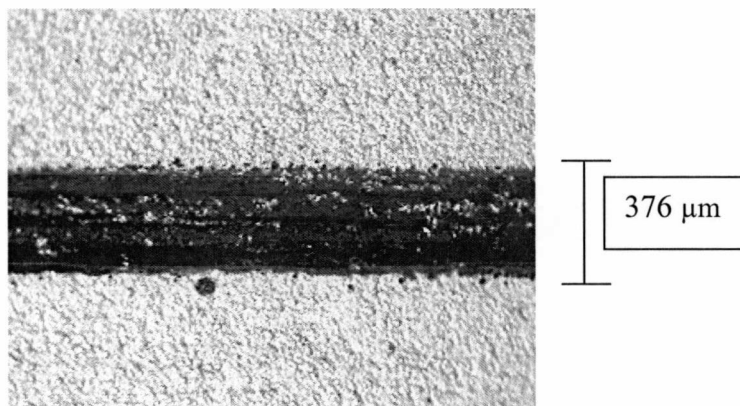


Figure 37: Wear track image for Ni- 7 g/L SiC sample

Table 12: Nickel only sample

Sample	Pure Ni Hexagonal sample
Pre-wear weight (g)	1.1356
Normal Force applied (N)	5.1
WC ball diameter (mm)	1389
Weight prior to wear	1.1356 grams
Total Wear Test Duration	~ 11minutes
Motor RPM	Varied
Total number of cycles	~1280
Traveled distance/cycle	19mm
Total distance traveled	48.64 m
Traverse speed	Varied
Strain readout sensitivity	1 μ strain per mV output
Calibration rate	~24 mN/ μ strain
Frictional Force	Varied
Final Wear Width	490 μ m
Final Wear Depth	22 μ m
Density (mg/mm³)	8.9

Table 12 - Continued

Speed (RPM)	Duration (min)	Strain (μs)	Post-Wear Weight (g)	Wear Loss (g) at each step
25	4	130	1.1356	0.0000
60	2	100	1.1355	0.0001
100	2	23	1.1354	0.0001
200	1	17	1.1352	0.0002
300	1	13	1.1349	0.0003
360	1	9	1.1344	0.0005

Wear Loss (g) accumulative	Speed (mm/s)	Friction Force (mN)	Coefficient of friction	Wear Depth (μm)	Wear Width (μm)	Accum. Wear Vol. (mm^3)
0.0000	16	3138	0.62	0	0	0.000
0.0001	38	2414	0.47	4	210	0.011
0.0002	63	555	0.11	7	270	0.022
0.0004	127	410	0.08	10	340	0.045
0.0007	190	314	0.06	15	409	0.079
0.0012	228	217	0.04	22	490	0.135

Table 12- Continued

Total number of cycles	1280
Total Traveled Distance (m)	48.64
Total Wear Mass Loss (g)	0.0012
Total Wear Volume Loss (mm³)	0.135

Figure 38 shows the plot for friction force vs. sliding speed for Nickel only sample. This plot also has an inverse relationship for friction force and the sliding speed.

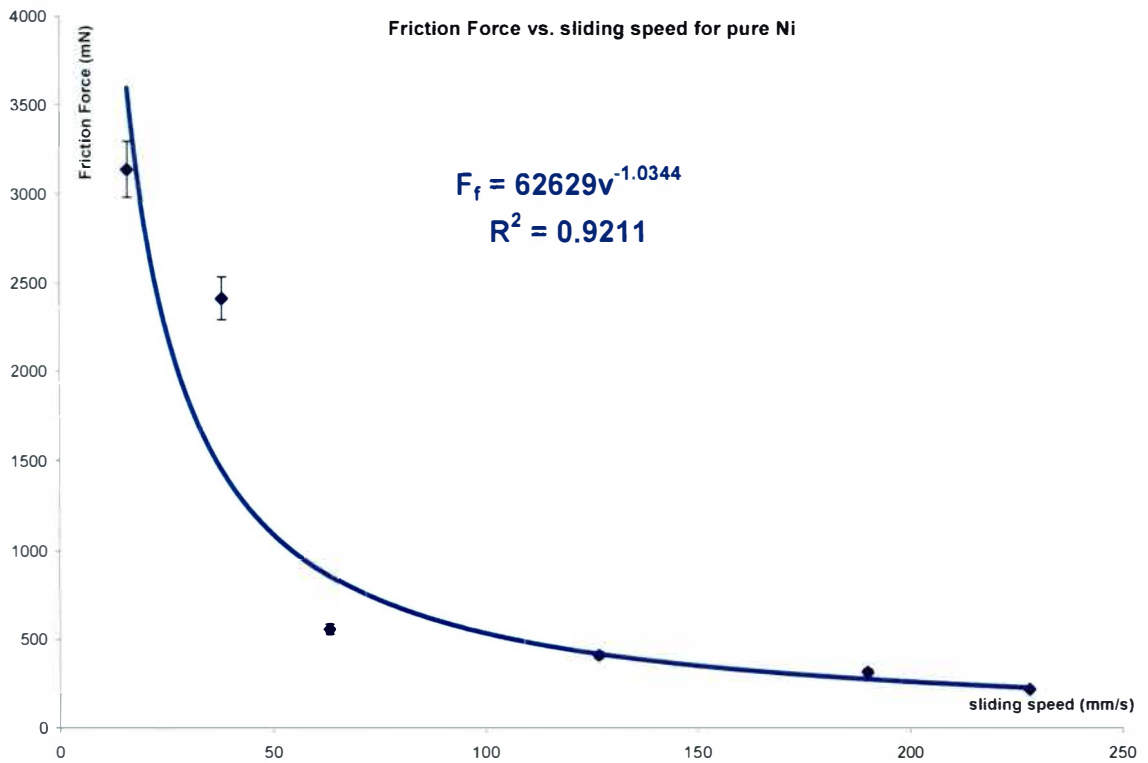


Figure 38: Friction force vs. sliding speed plot for Ni only sample

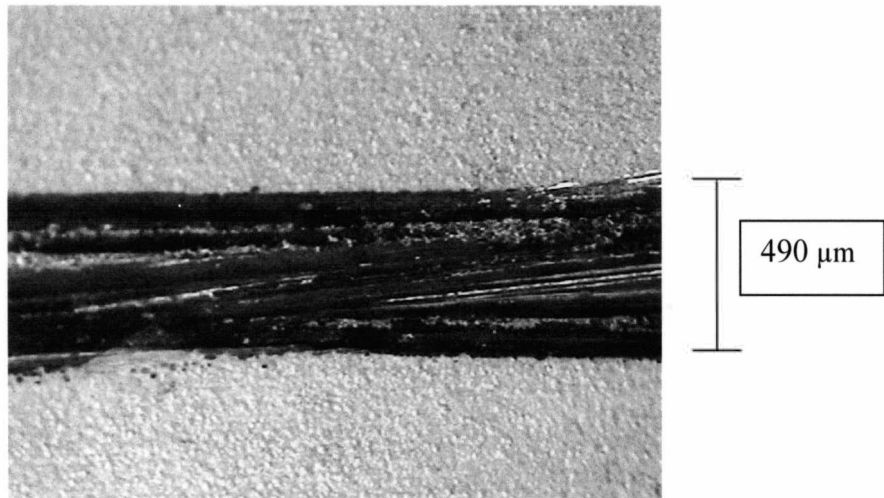


Figure 39: Wear track image for Ni only sample

Figure 40 below show the comparison of friction force vs. sliding speed for Ni-SiC and aluminum-Ni sample. It is inferred from the plot that the sliding speeds required for the Ni-SiC sample is more than that required for aluminum-Ni sample.

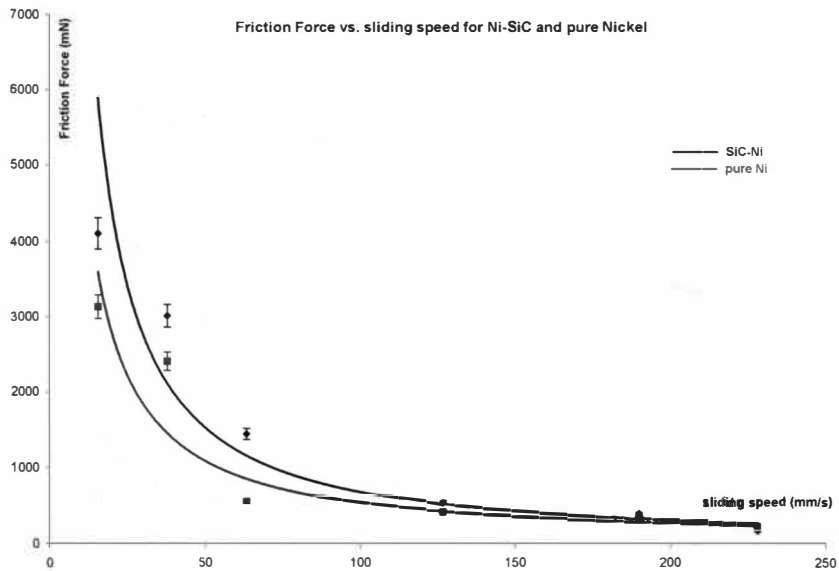


Figure 40: Comparison of friction force vs. sliding speed for Ni SiC and Ni only sample

Table 13: Nano silicon carbide specifications³¹

Particle Shape	Cubic
SiC wt%	98.9
Free C wt%	0.42
Total Al	0.02
Total Fe	0.02
Free SiO ₂	0.62
Average particle Size nm	50
Specific surface Area (m ² /g)	35±5
Compressed Bulk Density (g/cc)	1.93

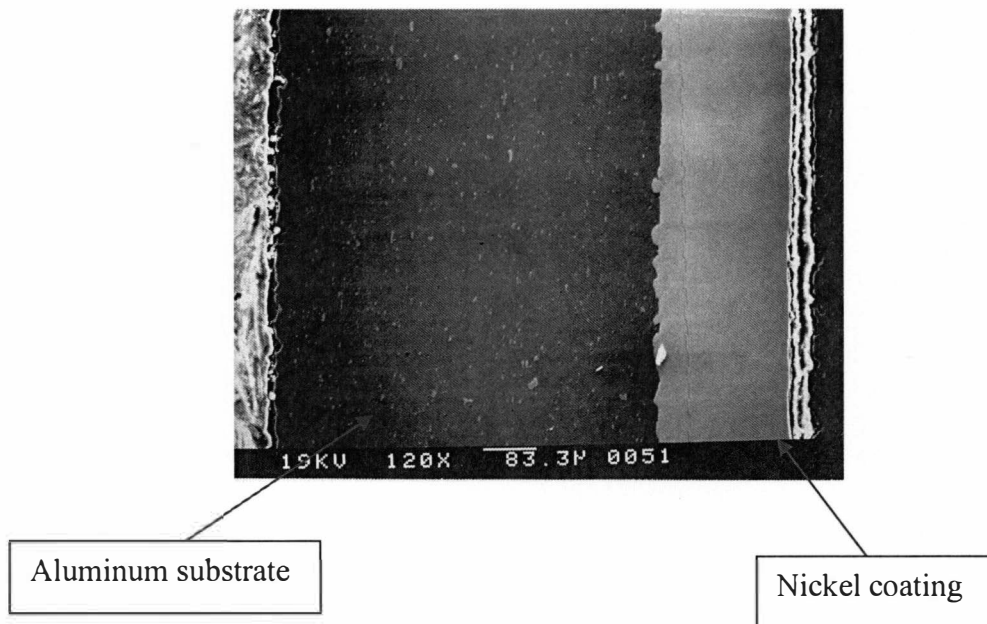


Figure 41: SEM micrograph 208 microns nickel coating

CHAPTER IV

DISCUSSION

- As seen from the results of residual stresses in the coating, from hole drilling and from bending due to stresses, it is evident that the stresses obtained for thick coatings (~200 μm) are tensile. Al-Khasawneh³⁰ got compressive values for 50 μm coating. This might be due to difference in time duration for the thicker coating and the coating thickness.
- The minimum and the maximum residual stresses as obtained from the hole drilling experiment are 152 MPa and 258 MPa respectively, and they decrease to a minimum and maximum of 68 MPa and 80 MPa respectively. These values fall in the range, 120 MPa to 296 MPa, as obtained by Stoney²⁴.
- The value obtained by calculating the bending due to tension, of the same 208 μm nickel coating, sample is 155 MPa. This value is in the range of 120 MPa to 296 MPa obtained by Stoney²⁴.
- From the potentiodynamic studies for corrosion in 0.6M NaCl, the corrosion rate of bare aluminum is highest followed by nickel coating of 208 microns and the lowest is nickel coating of 50 microns. The corrosion rate of the nickel -coated sample seems to be less than that of the bare aluminum, with the lowering of corrosion potential as evident from the results. Therefore it can be deduced that the nickel coated sample show a better resistance to

corrosion than the bare aluminum. Also because of the difference in the coating thicknesses, the corrosion resistance is hampered, as seen in 208 μm Ni coating. This is because larger thickness of the coating gives larger surface area at the edges, and more favorable sites for pitting corrosion.

- The main reason for lesser corrosion rate of 50 micron nickel coating, than the 208 microns of nickel coating, is the presence of nickel on the edges of the sample. This would have provided favorable sites for the initiation of pitting corrosion. Also the presence of tensile stresses in 208 μm Ni coating, and presence of compressive stresses³⁰ on 50 μm Ni coatings, may have had a pronounced effect on the corrosion resistance.
- From the results of the Young's modulus it is visible that the stiffness of the coated samples increases as we increase the amount of SiC in the coating bath. This is true for the compositions of 7 gm/L and 21 gm/L. But as we reach the results for 42 gm/L, the Young's modulus does not change much. This is likely to be due to the unchanged concentration of SiC particles in the coating itself. It seems like there is a critical composition for the addition of the nano-SiC in the coating bath, but this is not sufficient data to say that.
- The obtained value of the Young's modulus for aluminum, 72.3 GPa, is close to the theoretical value for aluminum which is 73 GPa.
- The wear test results obtained from the pin-on-reciprocating plate tribometer method give a clear indication, that the sample of Ni-SiC requires higher friction force when compared with the Ni only sample. Also the wear depth in the former sample the wear depth is lesser than that obtained from Ni only sample. This was expected because of high hardness of incorporated SiC

particles in the coating bath. This is also clearly evident from the comparison plots of both the samples. Friction coefficient for the composite sample Ni-SiC is also higher than that obtained for the Ni only sample. This is due to the surface roughness of the former sample due to the presence of nano-SiC present on the surface. The coefficient of friction for Ni only coating was 0.62, and for Ni-SiC coating was 0.8. This is in line with the results obtained by Shrestha⁶, wherein, the coefficient of friction for Ni only coating was 0.215 which increased to 0.225 with the addition of SiC particles. Also results obtained by Grosjean³¹, wherein the coefficient of friction for Ni only coating was 0.16 which increased to about 0.41 with the addition of SiC particles in the coating fall in the same line.

CHAPTER V

CONCLUSION

As evident from the residual stresses, wear tests, corrosion resistance and tensile test results, it can be said that coating 2024-T3 aluminum alloy with nickel has advantages in terms of better wear resistance and corrosion resistance. Adding the nano silicon carbide particles in the coating bath definitely increases the wear resistance and the stiffness of the aluminum alloy. Corrosion resistance tests and residual stress analysis should be conducted with the incorporation of nano SiC particles. It would be a good idea to conduct behavior study of the interface between the aluminum substrate and the nickel coating, because that will allow us to understand the interfacial strength of the coating better and also the development of stresses and preferred orientation at the interface.

REFERENCES

1. *Alcoa Structural Handbook* (1960). A Design Manual for Aluminum, Aluminum Company of America, Pittsburgh, PA.
2. Vilca, D.H., Moraes, S.R., Motheo, A.J. (2003). *Electrosynthesized Polyaniline for the Corrosion Protection of Aluminum Alloy 2024-T3*, Journal of the Brazilian Chemical Society, Brazil, v. 14, 52-58.
3. *Aluminum Alloy 2024-T3*, Retrieved November 18, 2009, from Utah State University website: http://www.neng.usu.edu/mae/faculty/stevef/info/MProp/Al_2024-T3.htm
4. Munger, C.G. (1985). *Corrosion Prevention by Protective Coatings*, National Association of Corrosion Engineers, Houston, Texas, 27-28.
5. Posmyk, A. (2003). *Influence of material properties on the wear of composite coatings*, Wear, vol.254, 399-407.
6. Shrestha, N. K., Masuko, M., Saji, T. (2003). *Composite plating of Ni/SiC using azo-cationic surfactants and wear resistance of coatings*, Wear, vol. 254, 555-564.
7. Benea, L., Bonora, P.L., Borello, A., Martelli, S. (2001). *Wear corrosion properties of nano-structured SiC-nickel composite coatings obtained by electroplating*, Wear, vol. 249, 995-1003.
8. Ted Guo, M. L., Tsao Chi. -Y. A. (2001). *Tribological behavior of aluminum/SiC/nickel-coated graphite hybrid composites*, Materials Science and Engineering A, vol. A333, 134-145.
9. Zimmerman, A. F., Clark, D. G., Aust, K. T., Erb, U. (2002). *Pulse electro deposition of Ni-SiC nanocomposite*, Materials letters, vol. 52, 2002, 85-90.

10. Edelstein, A. S., Cammarata, R.C. (1996). *Nanomaterials: synthesis, properties and applications*, Taylor & Francis Group, New York, NY.
11. Bari, G. D. (1994). *Nickel Plating*, ASM handbook, vol. 5, Surface Engineering, American Society for Metals, 201.
12. Cullity, B. D. (1978). *Elements of X-ray Diffraction*, second edition, Addison-Wesley, Reading, MA.
13. Hibbeler, R. C. (2002). *Mechanics of Material*, 5th edition, Macmillan, 83-86.
14. *Characteristics of a Stress- Strain Diagram*, Retrieved November 18, 2009, from University of Ottawa web:
<http://www.health.uottawa.ca/biomech/courses/pht1507/stress.pdf>
15. Breaux, N. J., Keska, J. K. (2002) *Application of a Pin-on-Disk Test to Determine Abrasive Wear*, American Society for Engineering, Proceedings of the 2002 ASEE Gulf-Southwest Annual Conference, University of Louisiana, March 20-22.
16. *Pin on Disc Tester*, Retrieved November 18, 2009, from Teer Coatings Limited website: <http://www.teercoatings.co.uk/index.php?page=podl>
17. Canning, W. (1970). *The Canning Handbook on Electroplating*, 21st edition, W Canning & Co. Ltd., Birmingham.
18. *Precoating sequence of 2024-T3 aluminum alloy*, Retrieved October 30, 2003, from metal finish glossary website: <http://www.iams.org/p2iris/metalfinish/1427-p.htm>
19. *Schematic of Electrochemical Cell*, Retrieved October 30, 2003, from University of Arizona website: <http://classes.engr.arizona.edu/mse110/Lab/Ecell.pdf>
20. Burns, R. M., Bradley, W. W. (1967). *Protective Coatings for Metals*, third edition, Reinhold Publication Corporation, 76-77.

21. Wang, S. C., Wei, W. C. J. (2003). *Kinetics of electroplating process of nano-sized ceramic particle/Ni composite*, Materials Chemistry and Physics, Vol. 78, 574-580.
22. Murakami, T., Gudczauskas, D., Liston, D. (2001). *High throwing powder nickel electroplating and its application*, 200th Meeting of the Electrochemical Society (Abstracts), San Francisco, CA.
23. *Measurement of Residual Stresses by Hole-Drilling Strain Gage Method*, TN-503-5, Retrieved October 30, 2003, <http://www.vishay.com/docs/11053/tn503.pdf>
24. Stoney, G. G. (1909). *The Tension of Metallic Films deposited by Electrolysis*, vol. A82, Proceedings of the Royal Society of London, 172-175.
25. Jain, A., Sinha, M. (1999). *A Comparative Study of Various Active and Passive Metals in Different Environments*, Senior Project, M.S. University, Vadodara, India.
26. *Corrosion Handbook*, National Association of Corrosion Engineers, Houston, TX, 2000.
27. Fontana, M. G., Greene, N. D. (1978). *Principles of Corrosion Engineering*, second edition, McGraw-Hill Book Co., New York.
28. *Glossary of Finishing Terms*, Retrieved October 30, 2003, from TechPlate website at: www.techplate.com/platingglossary1.htm
29. *Material Testing Systems*, Retrieved October 30, 2003, from Cornell University at: http://instructl.cit.cornell.edu/Courses/virtual_lab/chalktalks/materialtest/machine.pdf
30. Khasawneh, H. (2003). *Study of Residual Stress, Wear Test and Texture of Aluminum-Nickel Coating with/without Gamma Alumina and SiC particles*, Master's thesis, Western Michigan University, Kalamazoo, MI.

31. Grosjean, A., Rezrazi, M., Takadoum, J., Bercot, P. (2001). *Hardness, friction and wear characteristics of nickel-SiC electroless composite deposits*, Surface and Coatings Technology, vol. 137, issue 1, 92-96.

APPENDIX A

Suppliers

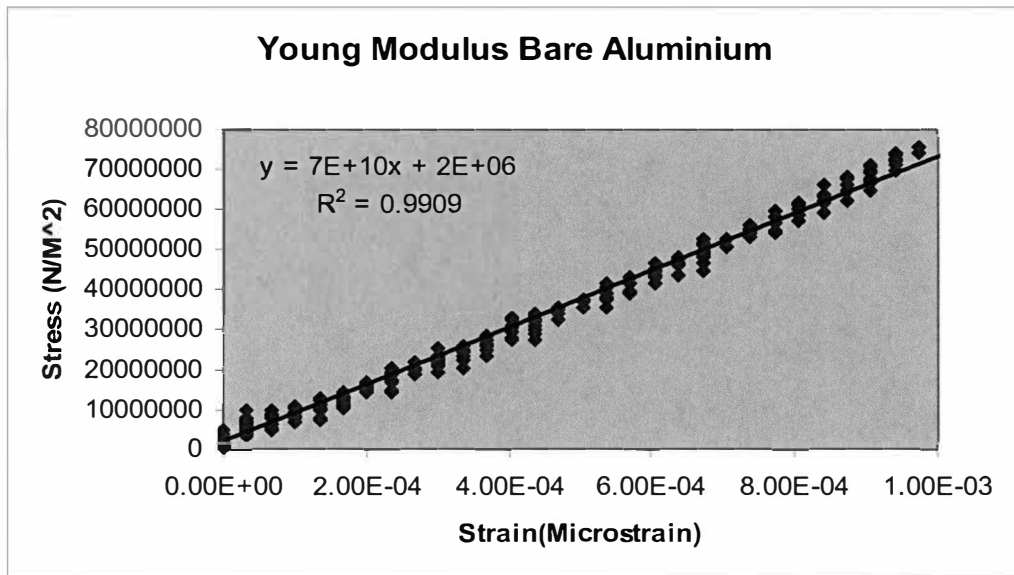
Item	Information	Supplier	Phone
Anode Bag	Plain Weave Polypro	Plating Products Inc.	1-765-457-1194
Immersion Heater	Vycor Quartz w/Cord and Plug 120V	VWR	1-800-932-4158 www.vwr.com
Al ₂ O ₃ Powder	1Kg	Nanophase Co.	1-630-323-1200 www.nanophase.com
Barrett-SN \$16.522/gallon \$82.61/5gallons	Nickel Sulfamate	MacDermid	1-800-325-4158 www.macdermid.com 513-984-8204 513-984-6400*114 Jennifer
Latex Glove Med		Chemistry Department	
HNO ₃ #33260 HCl #33257	Concentrated	Chemistry Department	Alfa Aesar --- \$196/ 2.5 liters (HCl) 41.70/ 6 pounds \$ 31.10/ pound (nitric acid) \$ 41.60/ 7 pounds Macdermid Nitric acid --- will email HCl----- will email
Flow Mater	100 SCFH Rotameter	Grainger	1-616-381-8500

Filters / REG & LUB	¼ "MINI Filter/REG & LUB"	Grainger	1-616-381-8500
Zincate	<u>Metex 6811</u> <u>\$20.58/gallon</u> <u>\$102.9/5 gallon pail</u>	MacDermid	1-800-987-3435 www.macdermid.com 513-984-8204 513-984-6400*114 Jennifer
Alkaline Degreaser		MacDermid	1-800-987-3435 www.macdermid.com 513-984-8204 513-984-6400*114 Jennifer
NaOH	Pure	Chemistry Department	
Al 2024-T3	0.635mm Sheet	Schupan Aluminum	1-269-382-3434 www.schupanalum.com
Anode	Nickel Oxide Depolarized Nickel	King Supply Allied	1-847-698-4564 1-800-241-0809
Coating Tank	Polypropylene Tank (305x305x304x12.7)	L.C. Fabricators.	1-908-241-4252 http://lcfab.hypermart.net
Coating Bath Heater	Teflon Heater, 1Kw 120V	L.C. Fabricators.	1-908-241-4252 http://lcfab.hypermart.net
D.C. Power Supply	100amp at 12 Volts output	L.C. Fabricators.	1-908-241-4252 http://lcfab.hypermart.net
SEM supplies		Focused resolutions	http://home.comcast.net/~microscopy/prod03.htm 1-978-689-3977
Carbon tape	21604 Gentry Lane, Brookeville, MD 20833	M.E. Taylor Engineering, Inc	http://www.semsupplies.com/Table%20of%20Contents.html 1-301-774-6246
Strain gages	CEA-06-062UW-350	Micro measurement s group	1-919-365-3800

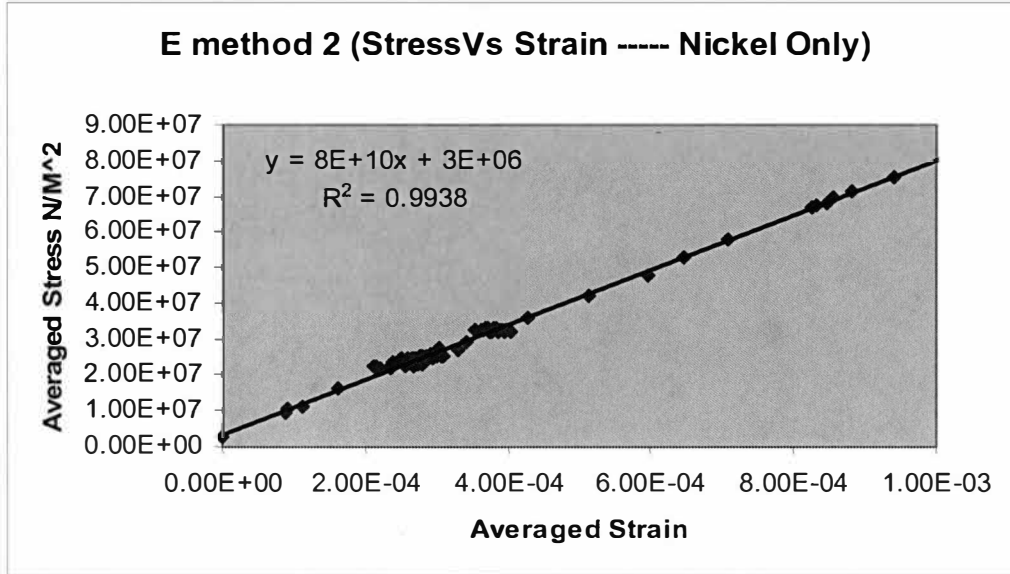
APPENDIX B

Tensile test plots

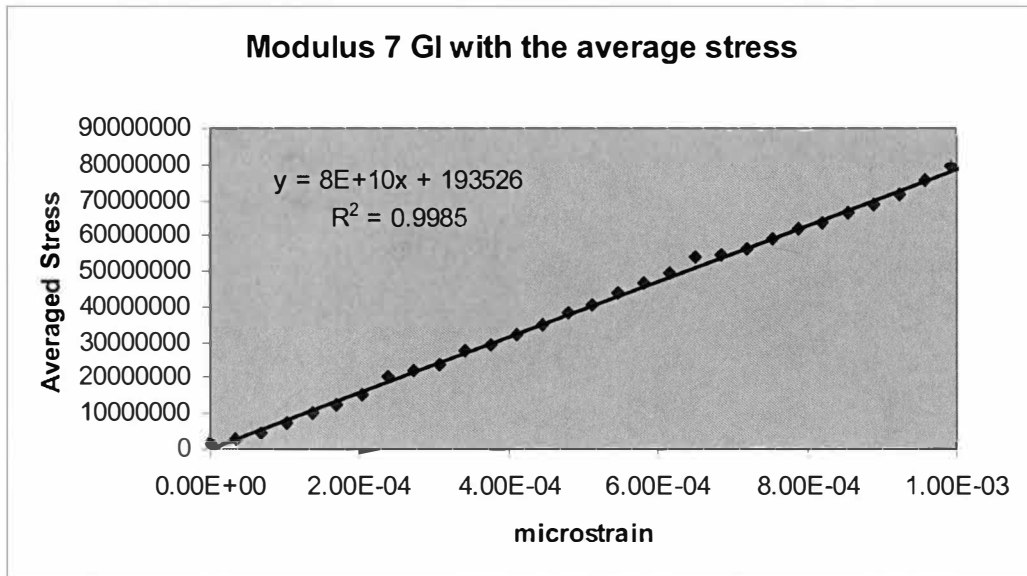
Bare Aluminum



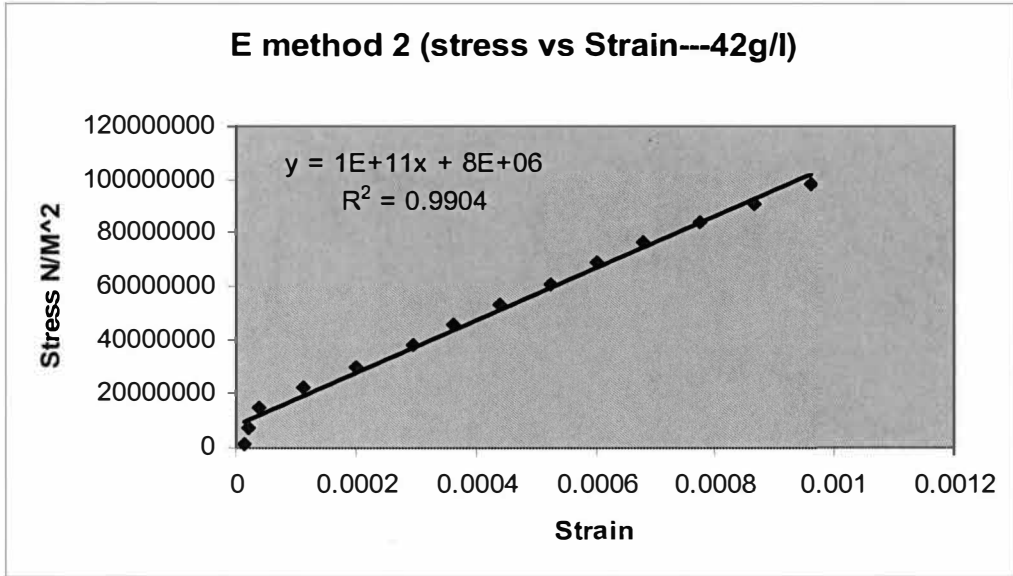
Aluminum – Nickel only coating



Aluminum – Nickel – 7 g/liter SiC (Method 1 Average stress)



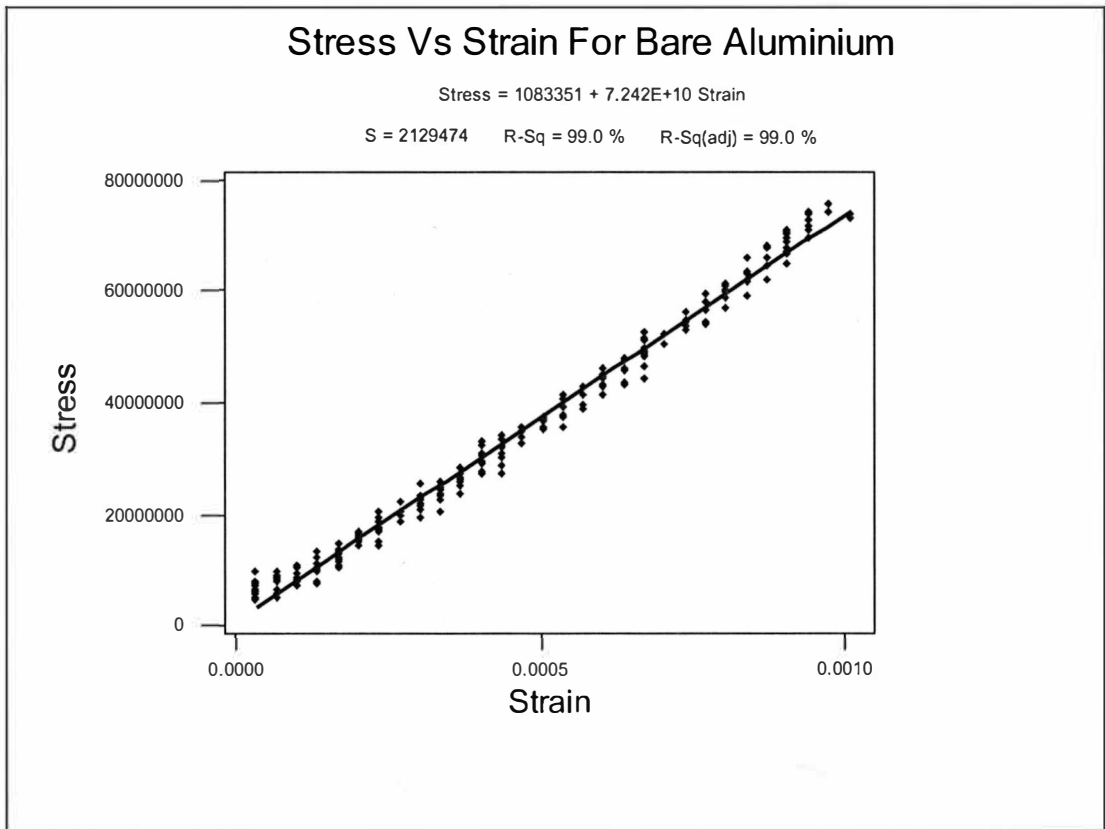
Aluminum – Nickel – 42 g/liter SiC



APPENDIX C

Minitab plots for tensile tests

Bare aluminum



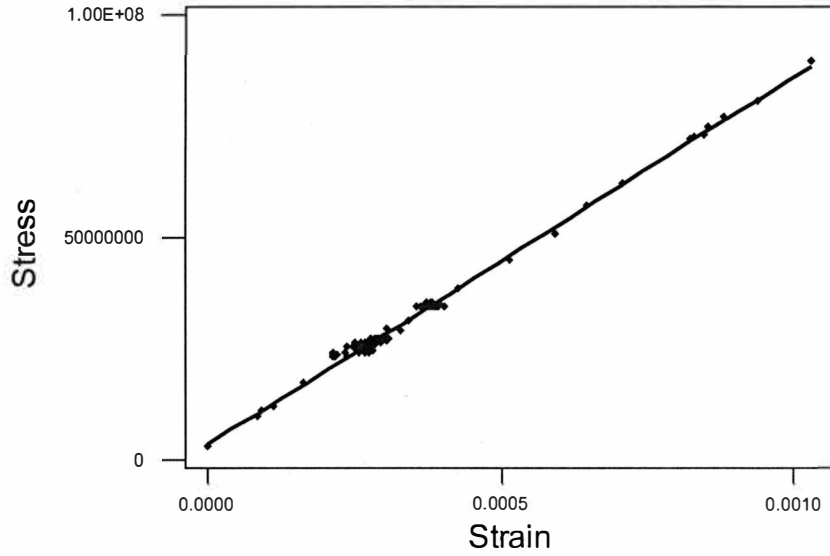
Young's Modulus = 72 GPa

Aluminum – nickel only

Stress Vs Strain For Nickel only

$$\text{Stress} = 3638198 + 8.223\text{E}+10 \text{ Strain}$$

S = 1080326 R-Sq = 99.4 % R-Sq(adj) = 99.4 %



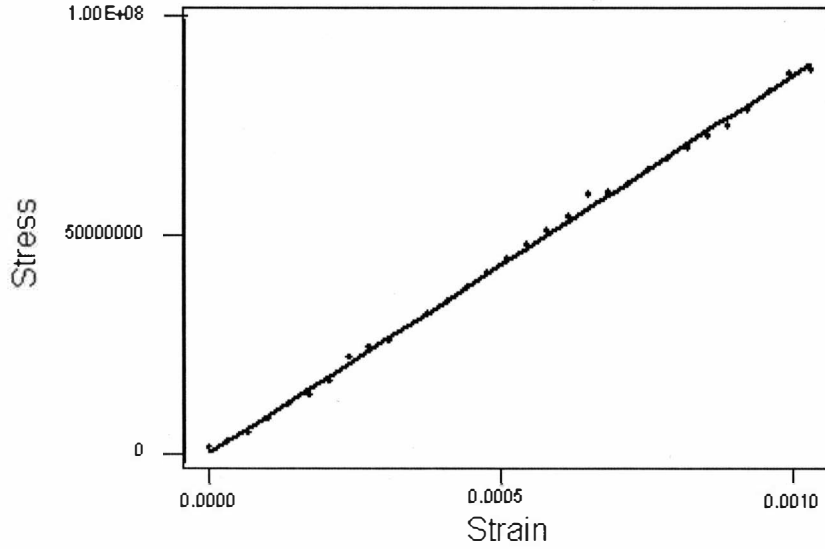
Young's Modulus = 82 GPa

Aluminum – nickel – 7g/liter SiC

Stress Vs Strain for 7g/ L

$$\text{Stress} = 206675 + 8.591\text{E}+10 \text{ Strain}$$

S = 1070069 R-Sq = 99.8 % R-Sq(adj) = 99.8 %



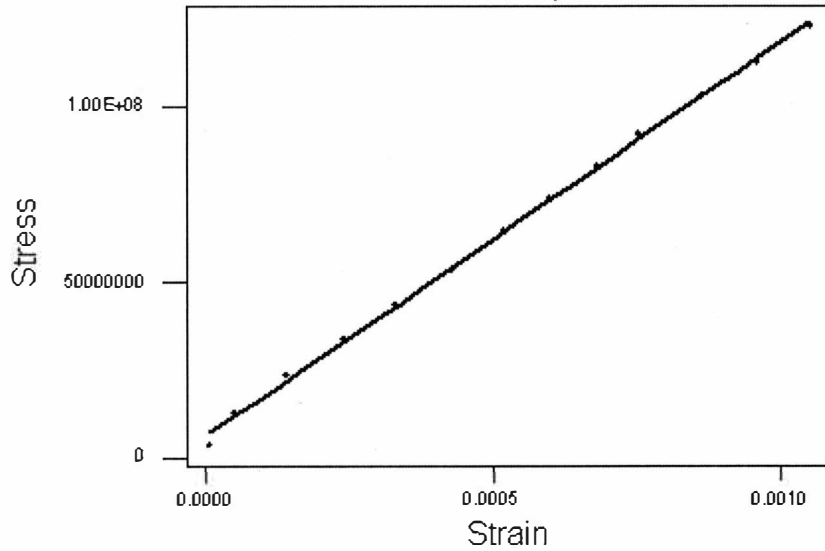
Young's Modulus = 86 GPa

Aluminum – nickel – 21g/liter SiC

Stress Vs Strain 21g/ L

$$\text{Stress} = 6587517 + 1.119\text{E}+11 \text{ Strain}$$

S = 1378028 R-Sq = 99.9 % R-Sq(adj) = 99.9 %



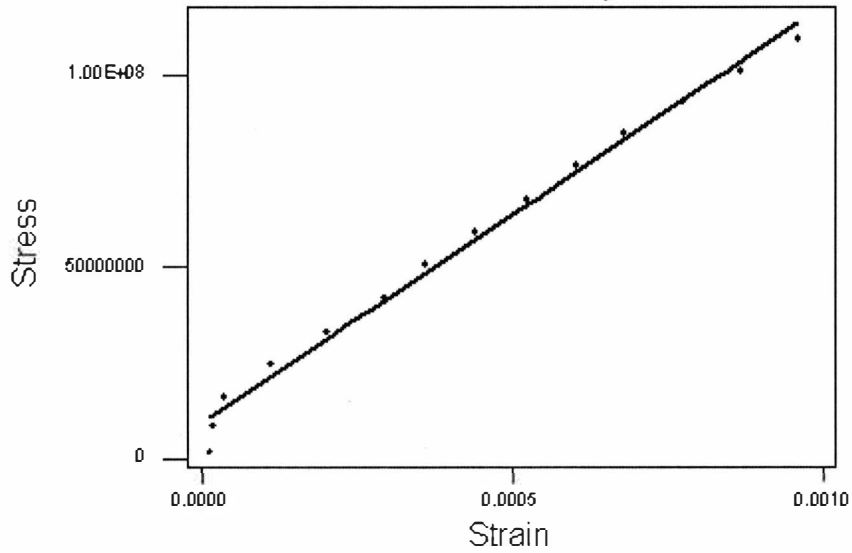
Young's Modulus = 112 GPa

Aluminum – nickel – 42g/liter SiC

Stress Vs Strain 42g/ L

$$\text{Stress} = 9320135 + 1.085\text{E}+11 \text{ Strain}$$

S = 3583320 R-Sq = 99.0 % R-Sq(adj) = 99.0 %



Young's Modulus = 109 GPa

BIBLIOGRAPHY

1. Juvinall, R. C. (1967). *Engineering Consideration of Stress, Strain, and Strength*, McGraw-Hill, New York.
2. Viktor, H., Behnken, H. (1997). *Structural and residual stress analysis by non-destructive methods: evaluation, application, assessment*, Elsevier, New York.
3. Bayer, R. G. (1994). *Mechanical Wear Prediction and Prevention*, Marcel Dekker, Inc. New York.
4. Burns, R. M., Bradley, W. W. (1967). *Protective Coatings for Metals*, third edition, Reinhold Publication Corporation.
5. Dennis, J. K., Such, T. E. (1972). *Nickel and chromium plating*, Butterworth & Co Ltd.
6. Parker, D. H. (1976). *Principles of Surface Coating Technology*, Wiley, NY.
7. Blum, W., Hogaboom, G. B. (1949). *Principles of Electroplating and Electroforming*” third edition, McGraw-Hill, New York.
8. Oettel, R. (2000). *The Determination of Uncertainties in Residual Stress Measurement (Using the hole drilling technique)*, Standards Measurement & Testing, Issue I.
9. Suresh, S., Giannakopoulos, A. E. (1998). *A new method for estimating residual stresses by instrumentation sharp indentation*, Acta Materialia, vol. 46, 5755-5767.

10. Prevey, P. S., *Current Applications of X-ray Diffraction Residual Stress Measurement*, Lambda Research, Lambda Technologies, Ohio.
11. Lord, J. (2000). *Hole Drilling Techniques*, BCA Structural Materials Workshop, National Physical Laboratory.
12. Cox, L. C. (1987). *Development of a Modified Blind Hole Test for the Measurement of Residual Stress Gradients in Thin Wear Resistant Coatings*, Proceedings of ASM's Conference on Residual Stress, ASM International.
13. Grosjean, A., Rezrazi, M., Takadoum, J., Bercot, P. (2001). *Hardness, friction and wear characteristics of nickel-SiC electroless composite deposits*, Surface and Coatings Technology, vol. 137, issue 1, 92-96.
14. Kim, S.K., Yoo, H. J. (1998). *Formation of bi-layer Ni-SiC composite by electrodeposition*, Surface and coatings technology, vol.108-109, 564-569.
15. Orlovskaja, L., Perience, N., Kurtinaitiene, M., Surviliene, S. (1999). *Ni-SiC composite under a modulated current*, Surface and coatings technology, vol. 111, 234-239.
16. Celis, J.P., Nowak, P., Socha, R.P., Kaisheva, M., Fransaer, J., Stoinov, Z. (1987). *Electrochemical investigation of the codeposition of SiC and SiO₂ particles with nickel*, Journal of Applied Electrochemistry, 1402-1408.
17. ASTM B 253-87, *Standard Guide for Preparation of Aluminum Alloys for Electroplating*, ASTM International.